Synchrotron radiation-based X-ray methods and vibrational spectroscopy techniques for the study of cultural heritage materials: a multi-method and multi-scale approach

Letizia Monico

CNR-Institute of Chemical Sciences and Technologies "Giulio Natta" (SCITEC) (Perugia, Italy)

letizia.monico@cnr.it

SCITEC

Consiglio Nazionale delle Ricerche

1-SR-based X-ray methods for cultural heritage objects*

➢ **Cultural heritage objects**: <u>heterogeneous and composite systems</u>, in the most of cases composed of <u>multiple layers</u>, whose thickness can achieve values of a few micrometers.

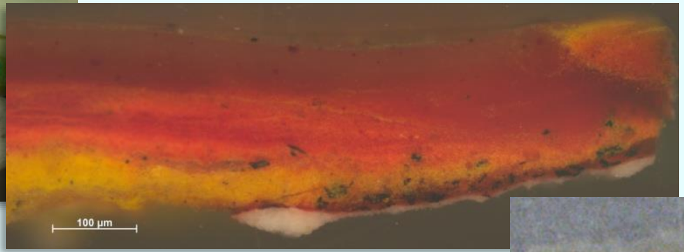

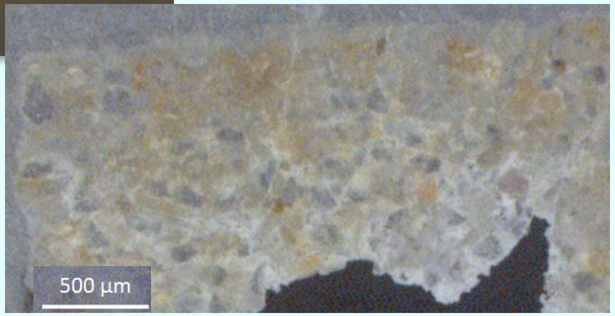

Subject to chemical transformations, often involving changes of the oxidation state of elements and formation of polymorphs.

➢ **SR-based X-ray methods (imaging/mapping and single-point analysis mode):** possibility of obtaining information about the chemical nature and distribution of different phases down to the sub-micrometer scale length.

a) **micro-X-ray fluorescence (µ-XRF)** for elemental microanalysis down to the sub-ppm level.

b) **micro-X-ray absorption spectroscopy (µ-XAS)** for probing the local chemical environment (oxidation state, coordination numbers, site symmetry and distortion, bond distances) of selected elements; it can be equally applied on amorphous or crystalline materials.

c) **micro-X-ray diffraction (µ-XRD)** for obtaining long range order information about the presence and nature of crystalline phases.

* M. Cotte *et al.*, *Accounts of chemical research* 43 (2010) 705-714; L. Bertrand *et al.*, *Appl. Phys. A* 106 (2012) 377–396; K. Janssens *et al.*, *Annu. Rev. Anal. Chem.* 6 (2013) 399–425; K. Janssens *et al.*, *Top. Curr. Chem.* 374(6) (2016), doi:10.1007/s41061-016-0079-2; M. Cotte *et al.*, *JAAS* 32 (2017) 477–493; V. Gonzalez *et al.*, *Chem. Eur. J.* 26 (2020) 1703 –1719; S. Quartieri, Synchrotron Radiation in Art, Archaelogy and Cultural Heritage. In *Synchrotron Radiation - Basics, Methods and Applications* (S. Mobilio, F. Boscehrini, C. Meneghini Eds.), Springer (2015), pp. 677-695.

1-Case studies and SR facilities

Alteration mechanism of pigments in oil paintings

- discoloration of cadmium yellows
- darkening of chrome yellows
- fading of Prussian blue

Color change due to redox processes

ID21/ID26 beamline

Marine Cotte
Wout De Nolf
Lucia Amidani
Pieter Glatzel

P06-PETRA III beamline

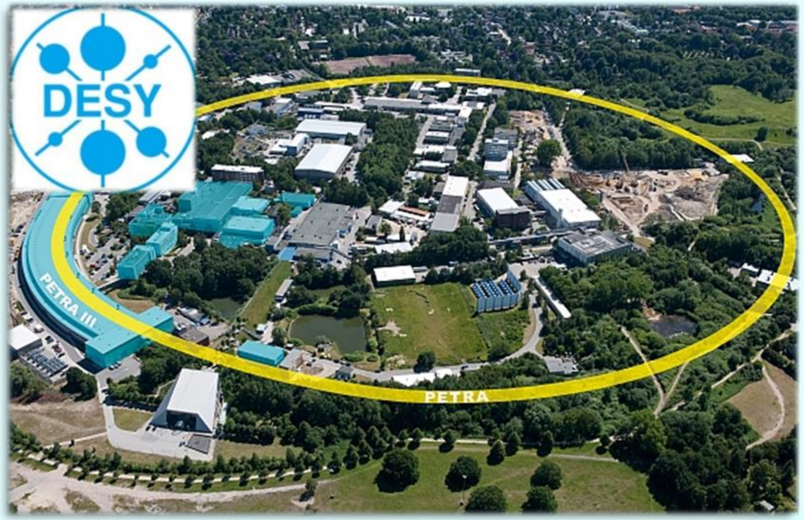

Gerald Falkenberg
Jan Garrevoet

XFM beamline

Daryl Howard

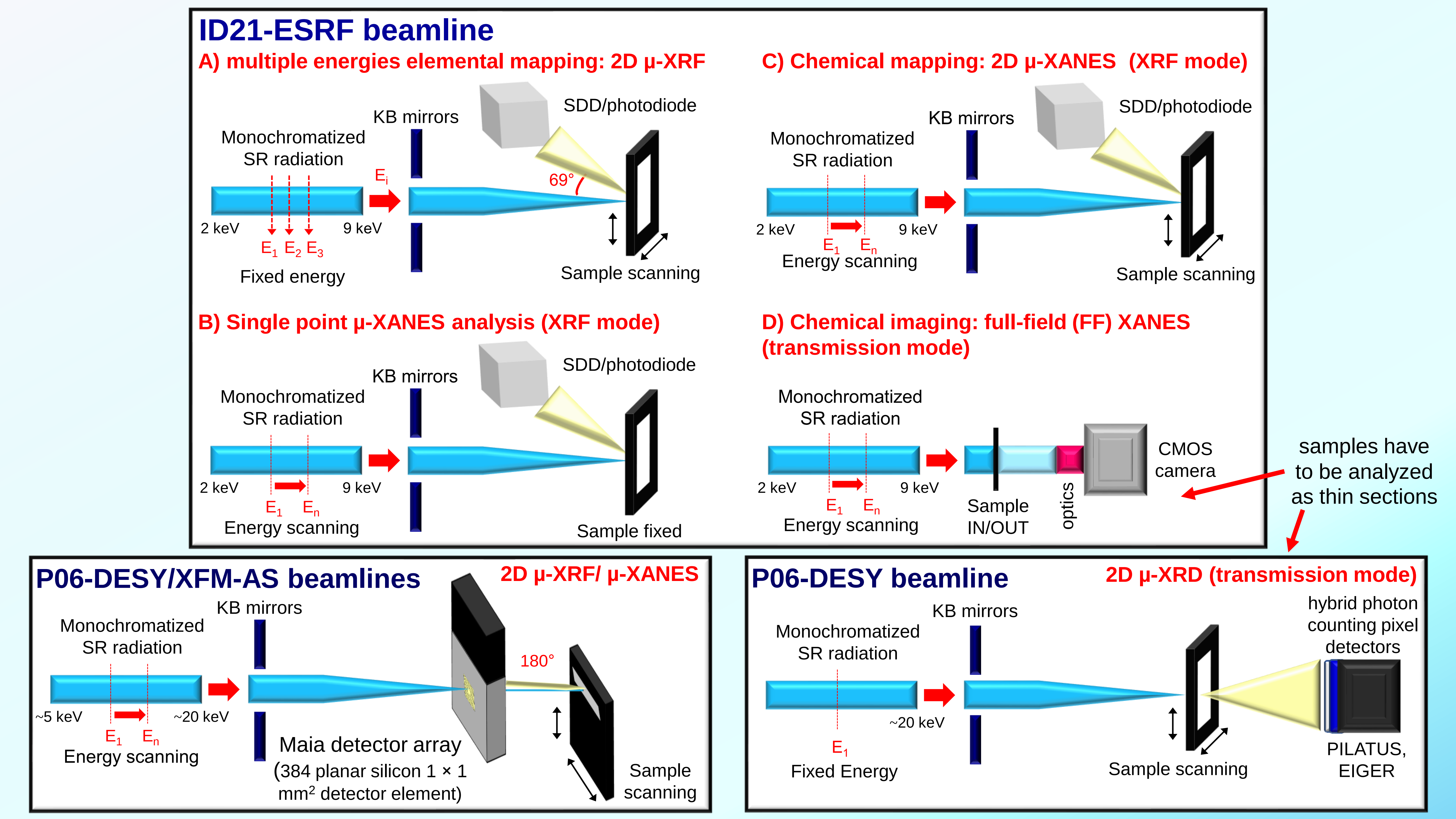

ID21-ESRF beamline
A) multiple energies elemental mapping: 2D μ-XRF
Monochromatized SR radiation
KB mirrors
SDD/photodiode
E_i
69°
2 keV
9 keV
E_1 E_2 E_3
Fixed energy
Sample scanning
C) Chemical mapping: 2D μ-XANES (XRF mode)
Monochromatized SR radiation
KB mirrors
SDD/photodiode
2 keV
9 keV
E_1 E_n
Energy scanning
Sample scanning
B) Single point μ-XANES analysis (XRF mode)
Monochromatized SR radiation
KB mirrors
SDD/photodiode
2 keV
9 keV
E_1 E_n
Energy scanning
Sample fixed
D) Chemical imaging: full-field (FF) XANES (transmission mode)
Monochromatized SR radiation
2 keV
9 keV
E_1 E_n
Energy scanning
Sample IN/OUT
optics
CMOS camera
samples have to be analyzed as thin sections
P06-DESY/XFM-AS beamlines
2D μ-XRF/ μ-XANES
Monochromatized SR radiation
KB mirrors
~5 keV
~20 keV
E_1 E_n
Energy scanning
180°
Maia detector array (384 planar silicon 1 × 1 mm^2 detector element)
Sample scanning
P06-DESY beamline
2D μ-XRD (transmission mode)
Monochromatized SR radiation
KB mirrors
~20 keV
E_1
Fixed Energy
Sample scanning
hybrid photon counting pixel detectors
PILATUS, EIGER

1-XANES-XRF mapping/imaging experiments

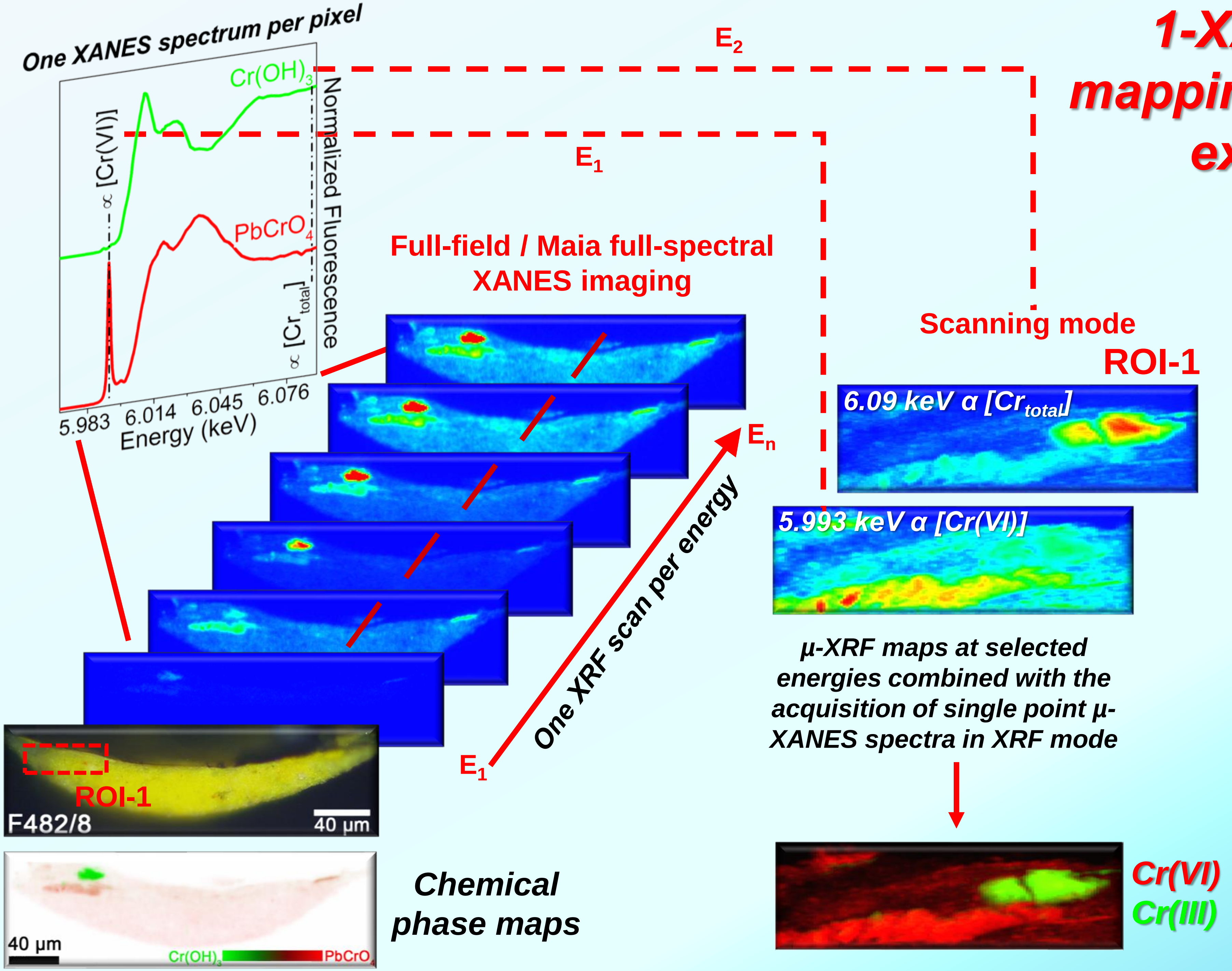

Alteration mechanism of pigments in oil paintings

2-Chromatic alteration of some yellow and blue pigments

Darkening of chrome yellows ($PbCr_{1-x}S_xO_4$)	Discoloration of cadmium yellows ($CdS/Cd_{1-x}Zn_xS$)	Fading of Prussian Blue [$MFe^{III}[Fe^{II}(CN)_6]\cdot xH_2O$, M= K^+, NH_4^+ or Na^+]

Sunflowers (V. van Gogh, 1889, Van Gogh Museum, Amsterdam)

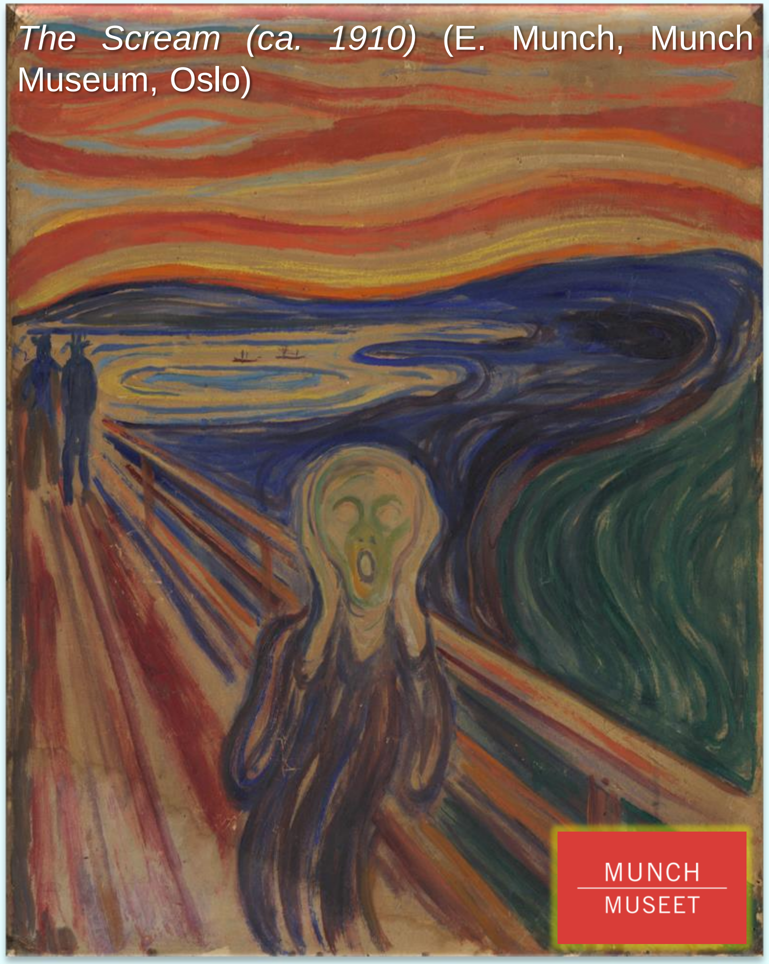

The Scream (ca. 1910) (E. Munch, Munch Museum, Oslo)

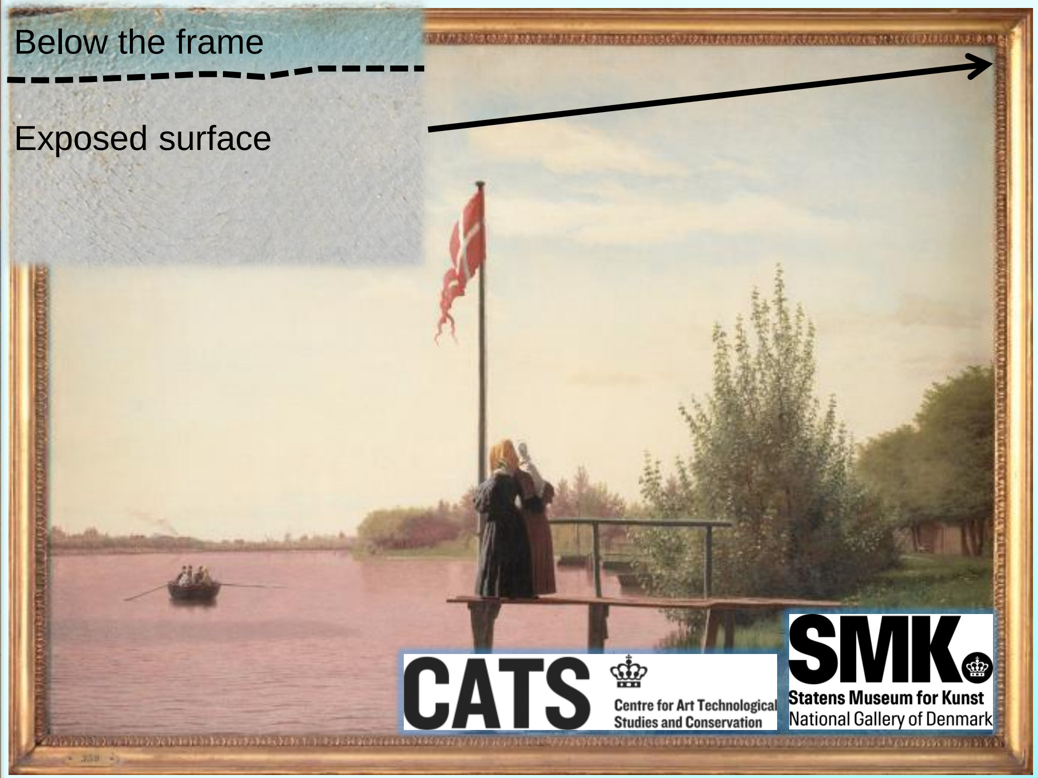

View of Lake Sortedam from Dosseringen Looking Towards the Suburb Nørrebro outside Copenhagen (Christen Købke, 1838, Statens Museum for Kunst, Copenhagen)

Why **and** ***how*** **such alteration processes take place?**

- ➢ Developing strategies to prevent/mitigate the degradation processes
- ➢ Optimizing strategies for the long-term conservation of paintings

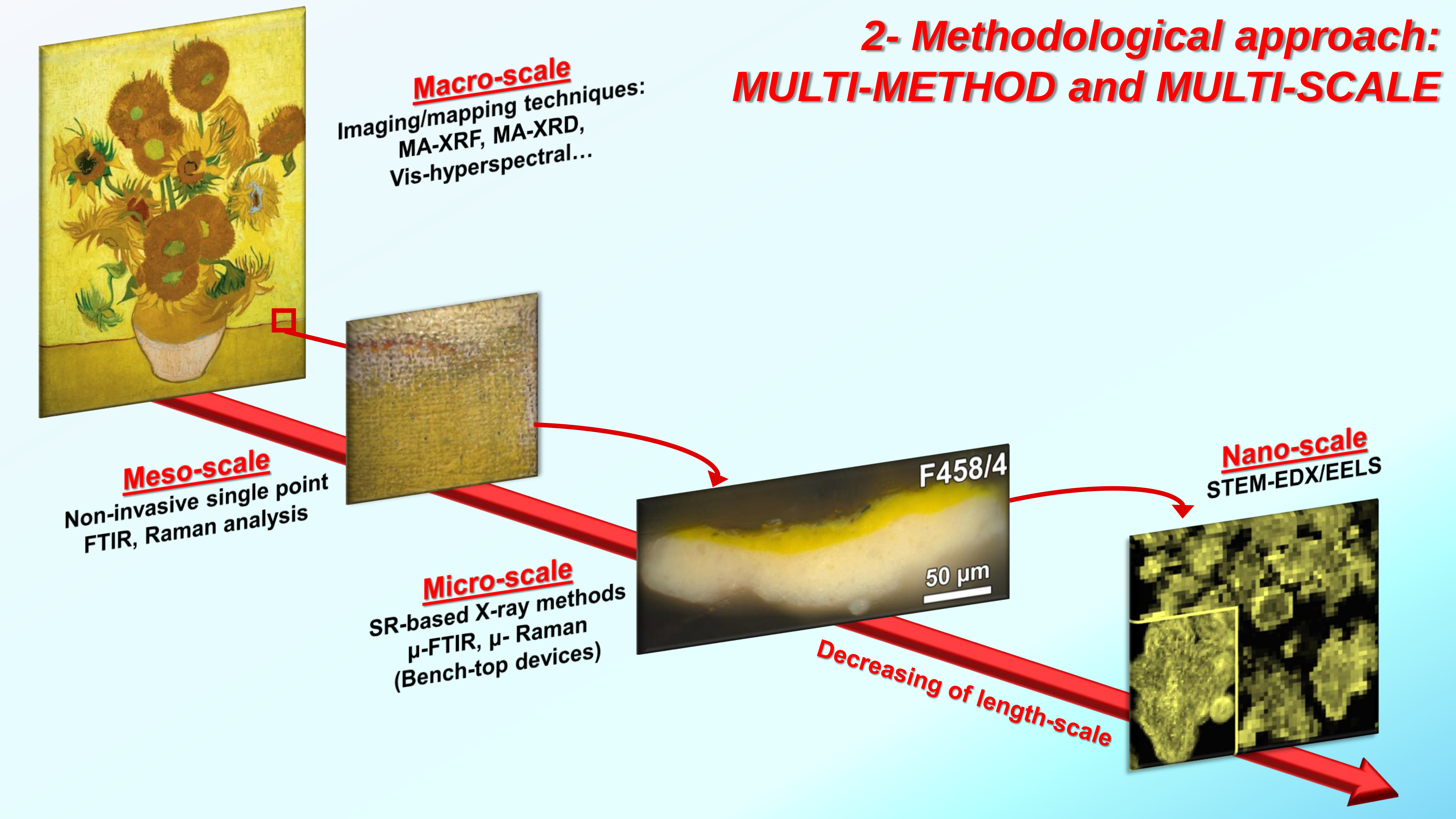
2- Methodological approach:
MULTI-METHOD and MULTI-SCALE
Macro-scale
Imaging/mapping techniques:
MA-XRF, MA-XRD,
Vis-hyperspectral…
Meso-scale
Non-invasive single point
FTIR, Raman analysis
Micro-scale
SR-based X-ray methods
μ-FTIR, μ- Raman
(Bench-top devices)
F458/4
50 μm
Nano-scale
STEM-EDX/EELS
Decreasing of length-scale

2- Methodological approach: MULTI-MATERIAL

Study of pigments and paint mock-ups

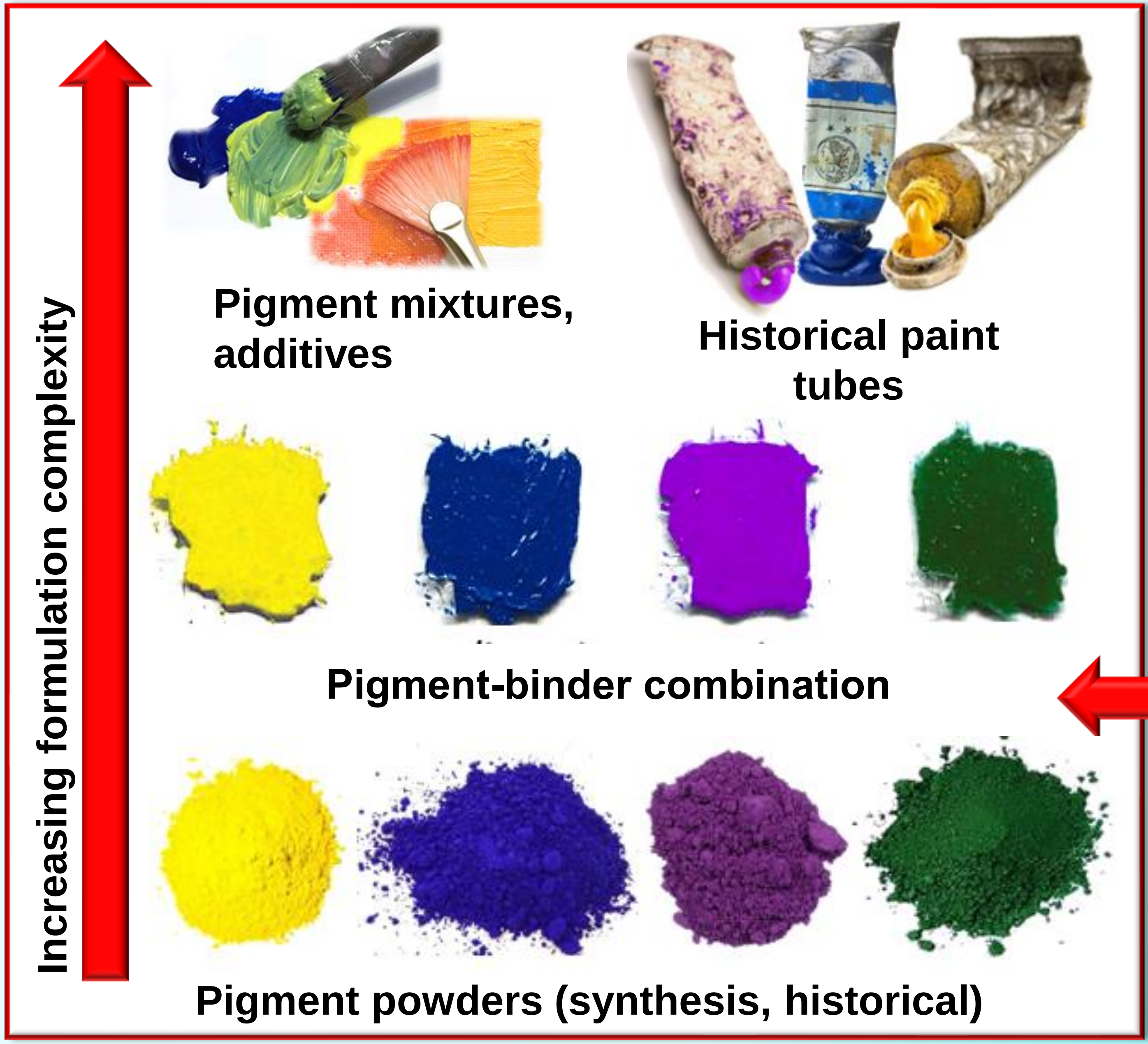

Paint materials:
Dynamic-complex systems

Interaction with the environment
- light
- humidity
- temperature

Discoloration of cadmium yellows

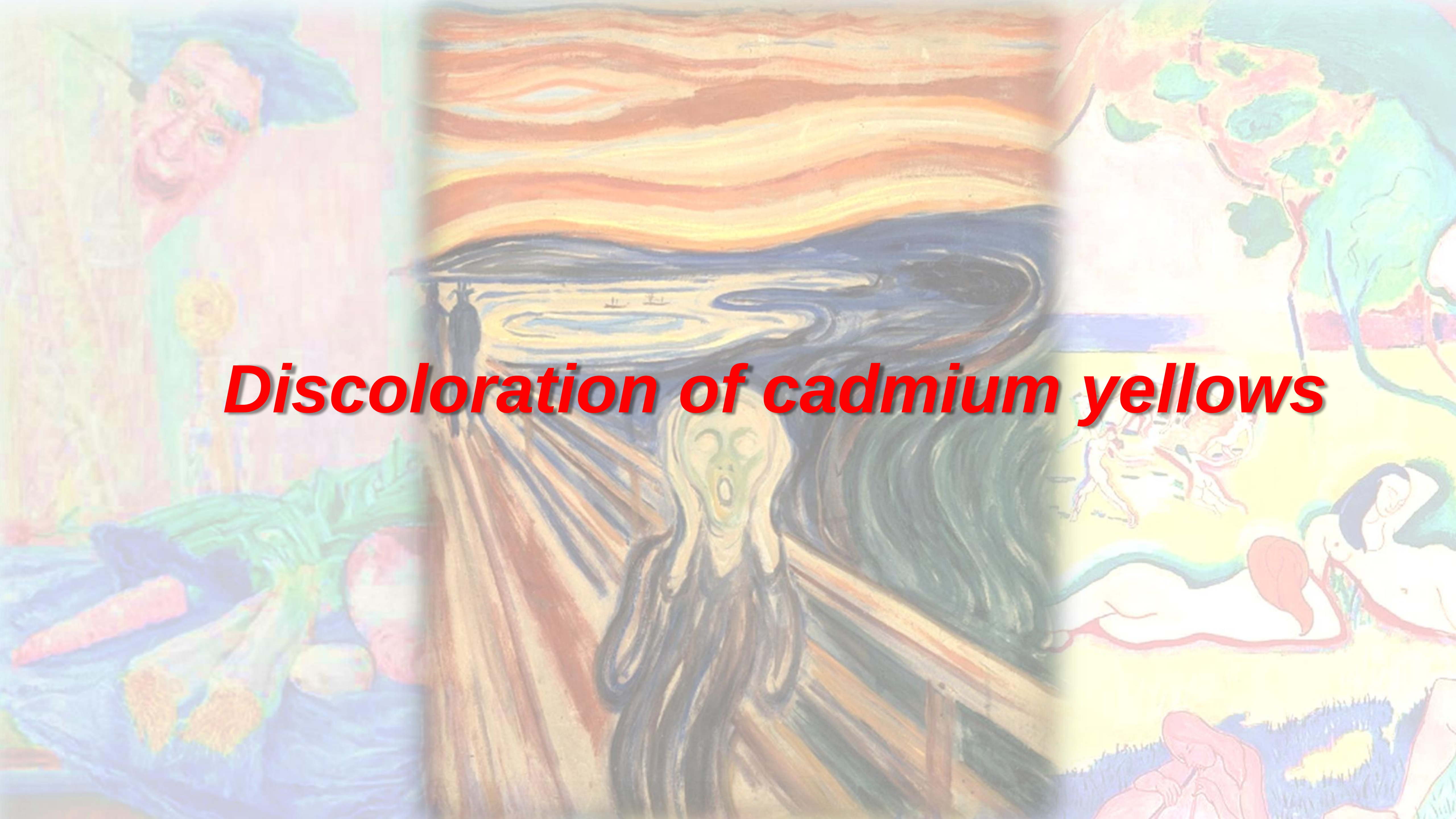

3-Discoloration of cadmium yellows ($CdS/Cd_{1-x}Zn_xS$)

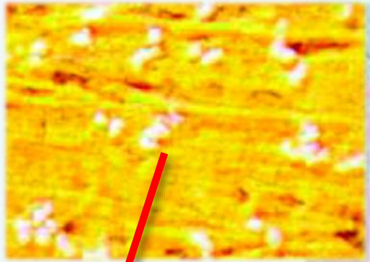

White globules at the exposed yellow paint surface

Still Life with Cabbage (James Ensor, ca. 1921, Kröller-Müller Museum, Otterlo, NL) [(a)]

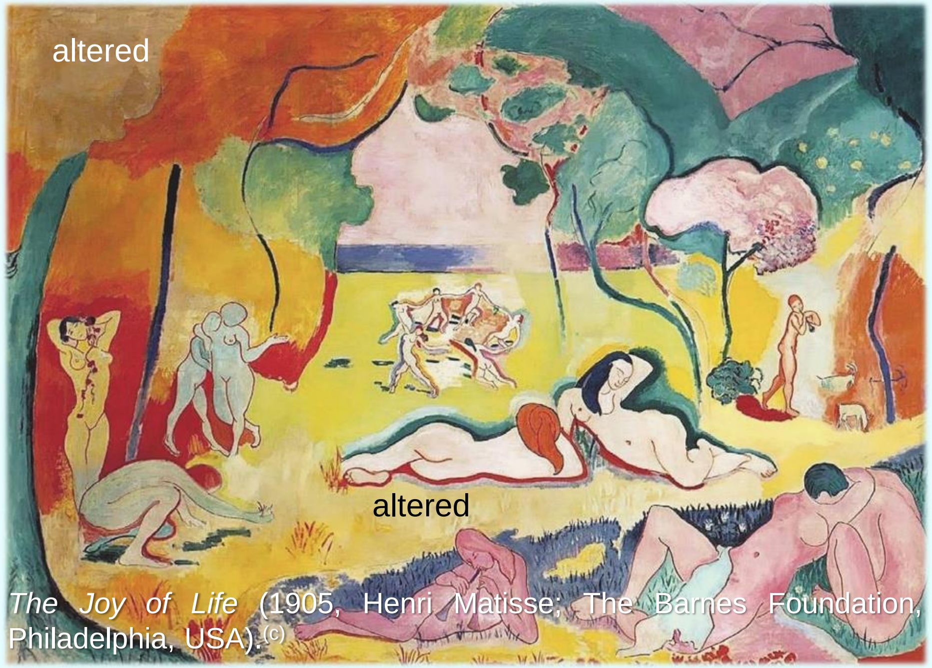

The Joy of Life (1905, Henri Matisse; The Barnes Foundation, Philadelphia, USA).[(c)]

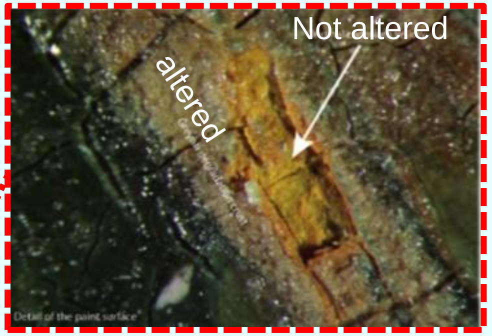

Flowers in a blue vase (1887, V. van Gogh; Kröller-Müller Museum, Otterlo).[(b)]

Artificially aged oil paint mock-ups[(d)]

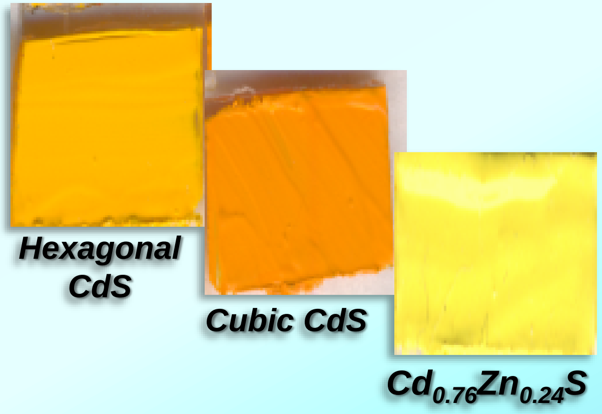

- Oxidation process triggered by light and humidity[(d)]

$$\mathbf{CdS} + 4h^{+}_{surf} + 2\,H_2O + O_2 \rightarrow \mathbf{CdSO_4} + 4H^{+}$$

- Formation of additional secondary products

$CdSO_4 \cdot H_2O$, zinc and cadmium oxalates, $(NH_4)_2Cd(SO_4)_2$

[(a)] G. Van der Snickt *et al., Anal. Chem.*, 81 (2009) 2600–2610; [(b)] G. Van der Snickt *et al., Anal. Chem.* 84 (2012) 10221-10228; [(c)] E. Pouyet *et al.*, *Applied Physics A* 121 (2015) 967-980; [(d)] L. Monico *et al.*, *Chem. Eur. J.* 24 (2018), 11584-11593.

3-The Scream (ca. 1910) by E. Munch

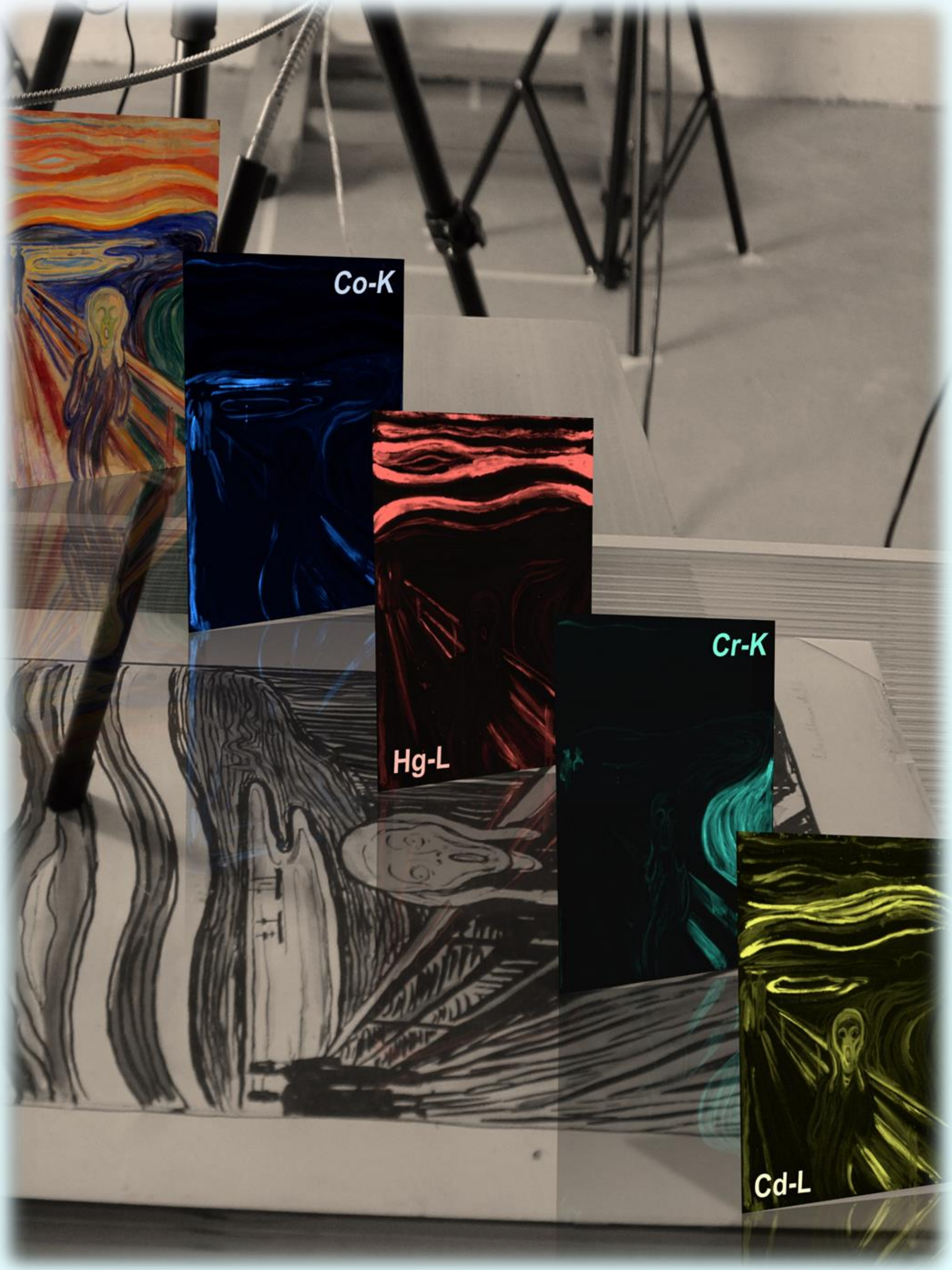

IPERION CH

MUNCH MUSEET

SCIENCE ADVANCES | RESEARCH ARTICLE

CHEMISTRY

Probing the chemistry of CdS paints in *The Scream* by in situ noninvasive spectroscopies and synchrotron radiation x-ray techniques

Letizia Monico[1,2,3]*, Laura Cartechini[1,2], Francesca Rosi[1,2], Annalisa Chieli[1,2], Chiara Grazia[1,2], Steven De Meyer[3], Gert Nuyts[3], Frederik Vanmeert[3], Koen Janssens[3,4], Marine Cotte[5,6], Wout De Nolf[5], Gerald Falkenberg[7], Irina Crina Anca Sandu[8], Eva Storevik Tveit[8], Jennifer Mass[9,10], Renato Pereira de Freitas[1,11], Aldo Romani[1,2], Costanza Miliani[1,2,12]*

Monico *et al.*, *Sci. Adv.* 2020; **6** : eaay3514   15 May 2020

3-Fading and flaking issues of cadmium yellow paints

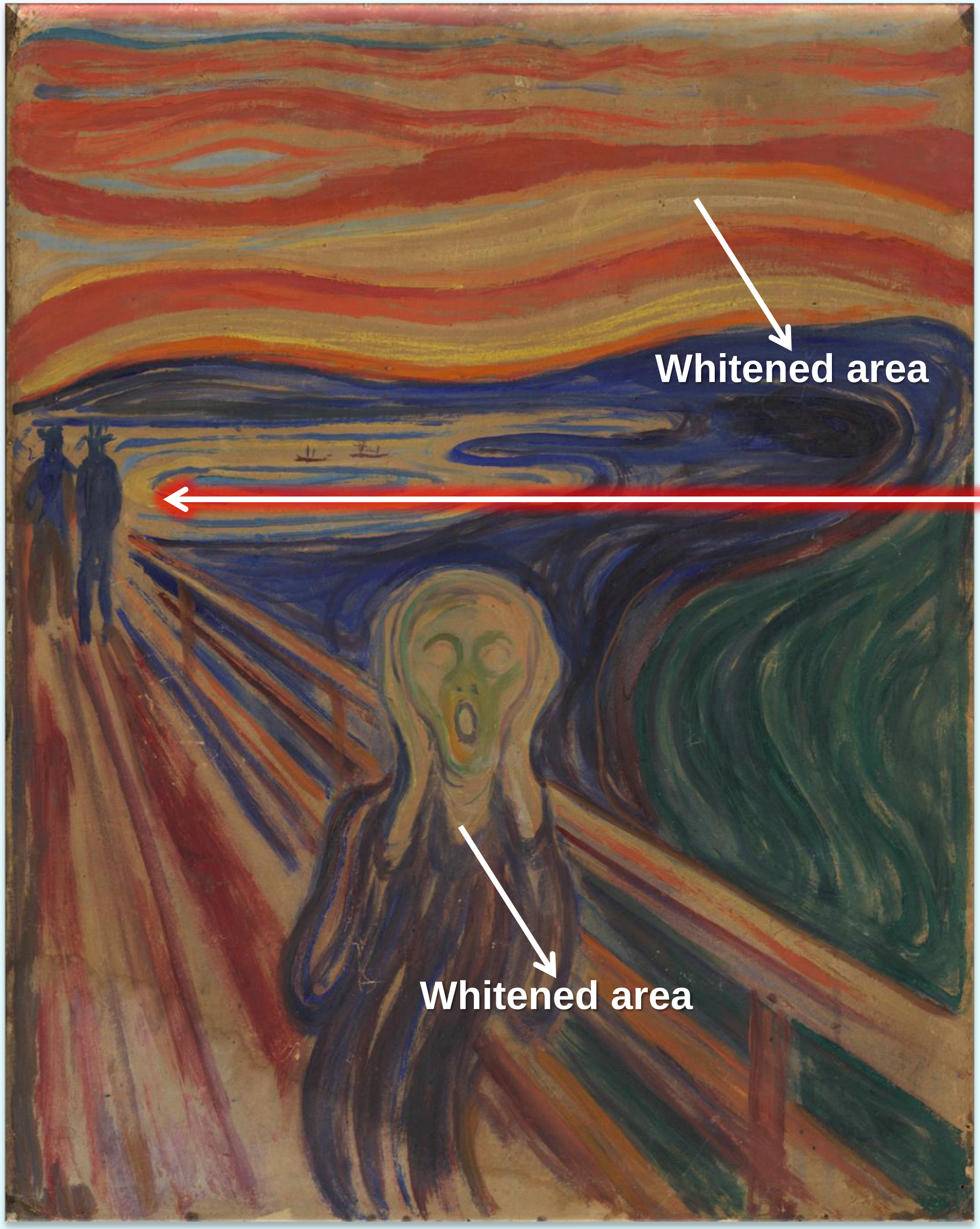

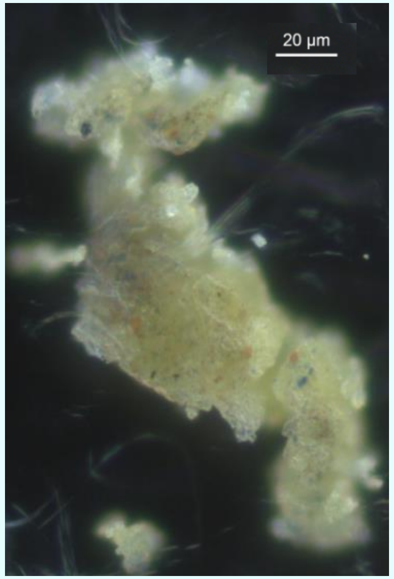

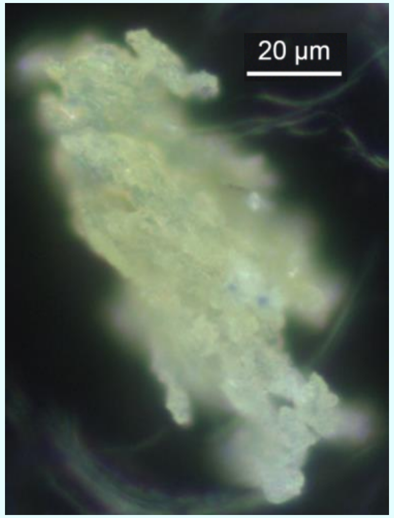

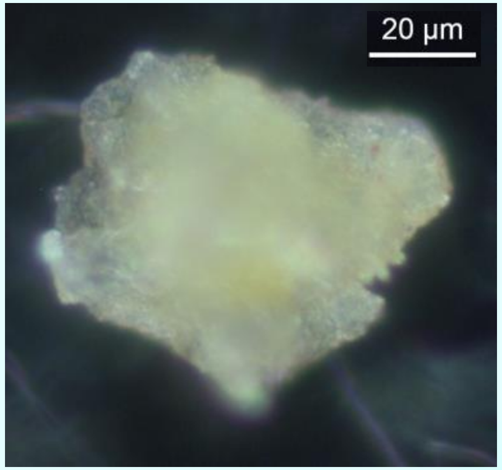

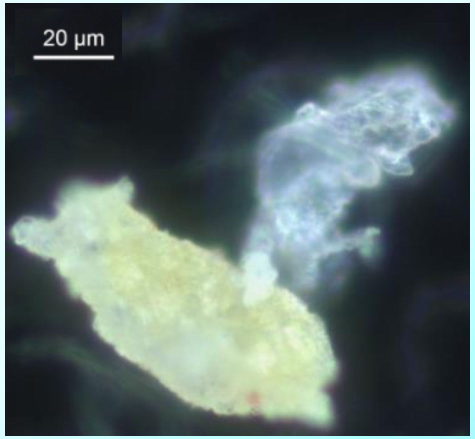

Analysis of a series of microflakes lost/fallen down from a flaked-off cadmium yellow area

L. Monico *et al.*, *Science Advances* 6 (2020), eaay3514

3-Evaluation of the effects of moisture and chloride-species

- What is the role of Cd-chloride compounds?

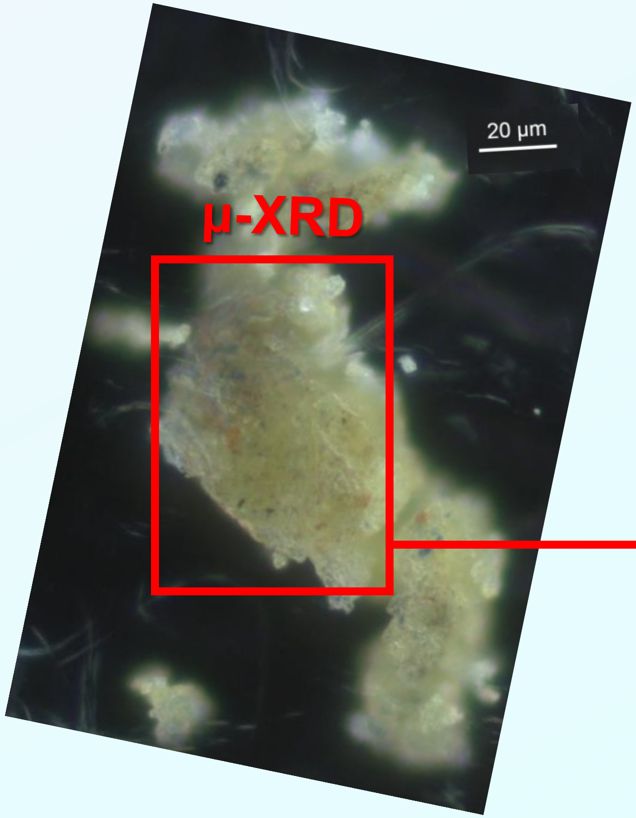

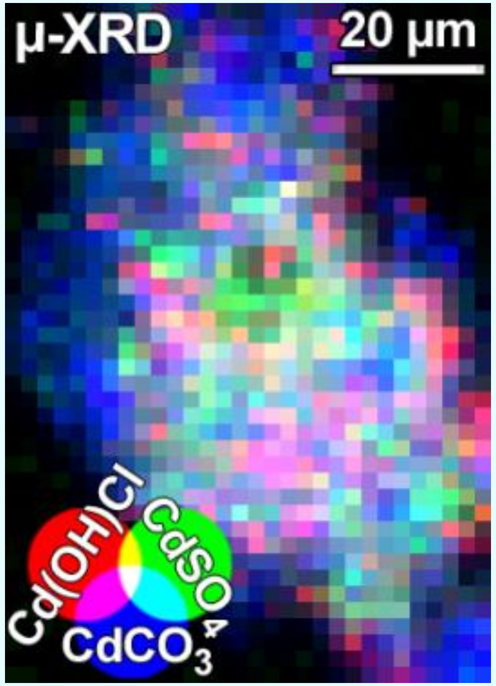

ESRF
ID21

Thermally aged oil paint mock-ups (RH≥95%, T=40°C)

- **Early 20th century historical powder (RCE collection, Amsterdam)**

Sample 7914

hex-CdS,
$CdCO_3$,
Cd(OH)Cl

- **Paint tube belonged to Munch (LF G 2.4, Munch Museum)**

CdS, $CdCO_3$, **CdCl-compounds**

L. Monico *et al.*, *Science Advances* 6 (2020), eaay3514

3-Early 20th century historical powder

Unaged ***Aged***

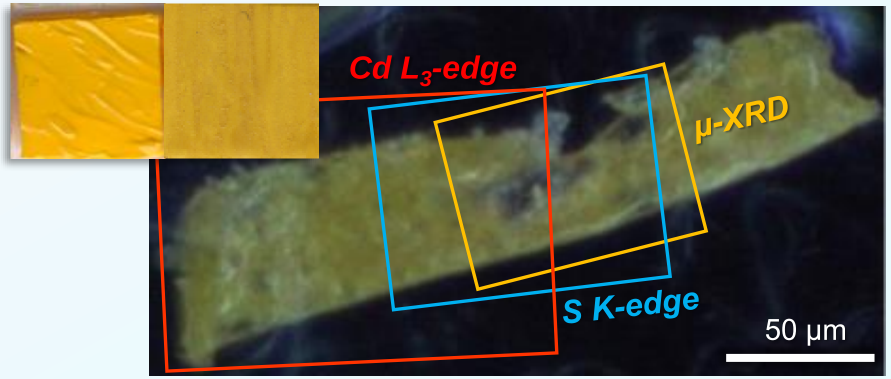

Thin section (thickness ~ 2µm)

µ-XRD (transmission mode)

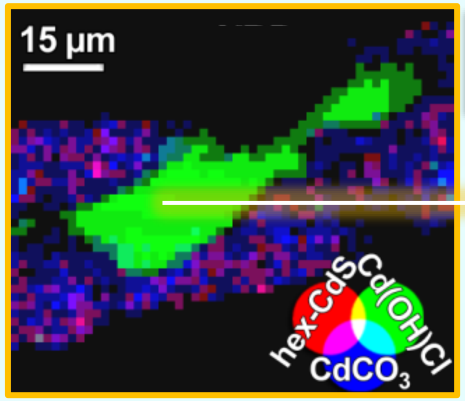

P06

Cd(OH)Cl
broadening of µ-XRD peaks: Nano-crystals.

Possible migration followed by precipitation during the $S^{2-} \rightarrow SO_4^{2-}$ oxidation

S K-edge (scanning mode)

ID21

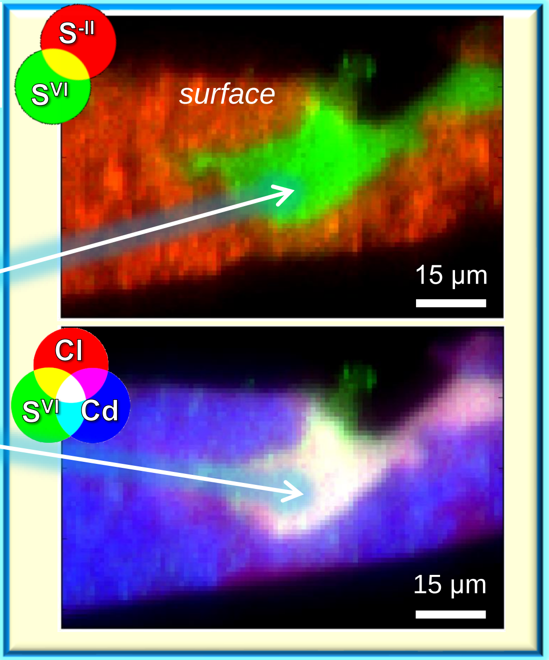

cadmium sulfate + sulfites

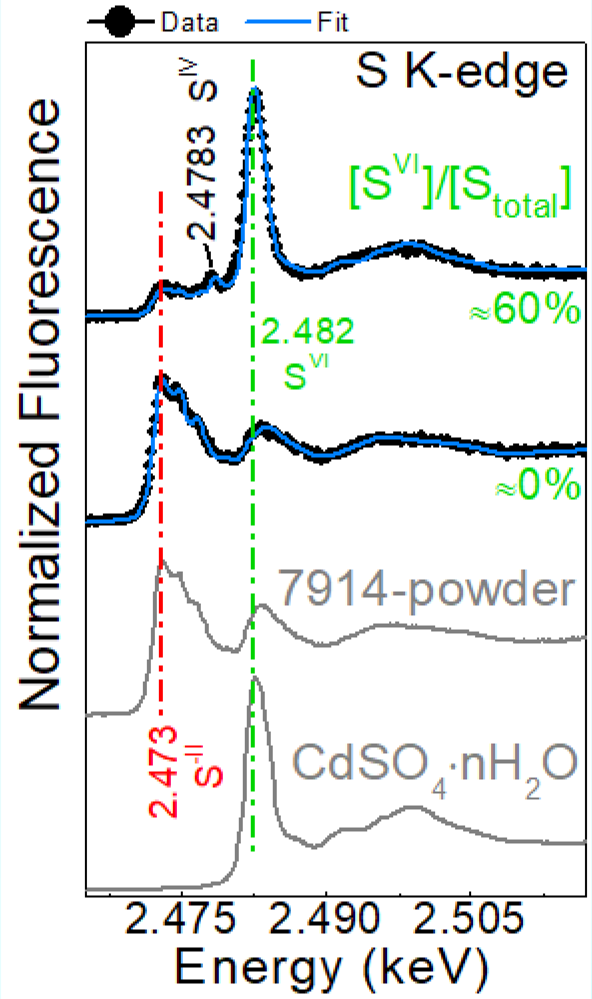

Cd L3-edge (full-field mode)

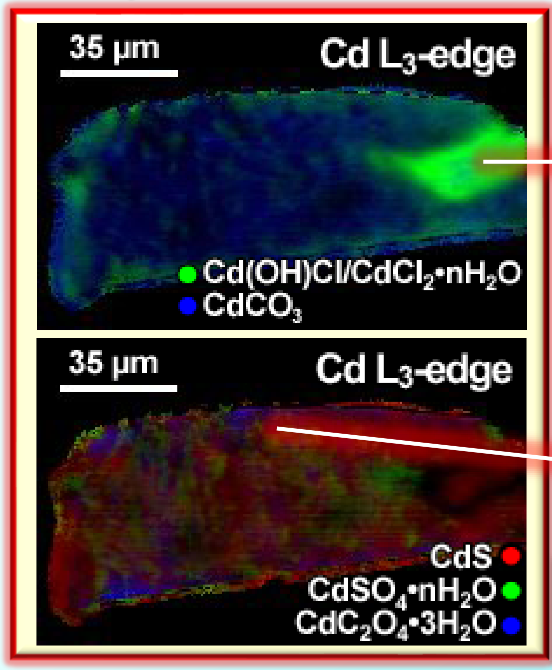

Cd-chlorides

Cd-oxalate

ID21

L. Monico *et al.*, *Science Advances* 6 (2020), eaay3514

3- Munch's paint tube (LF G 2.4)

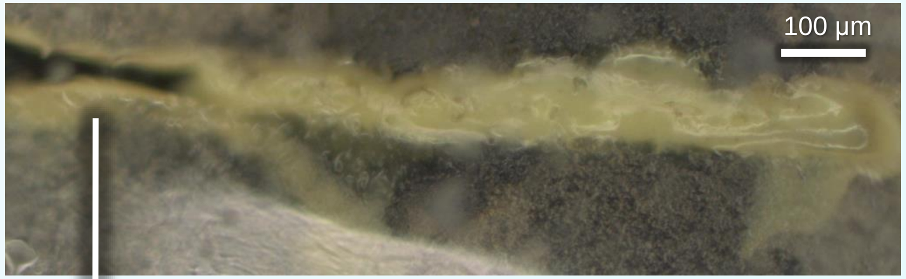

Thin section (thickness ~ 2µm)

ESRF
ID21

S K-edge full field-XANES imaging

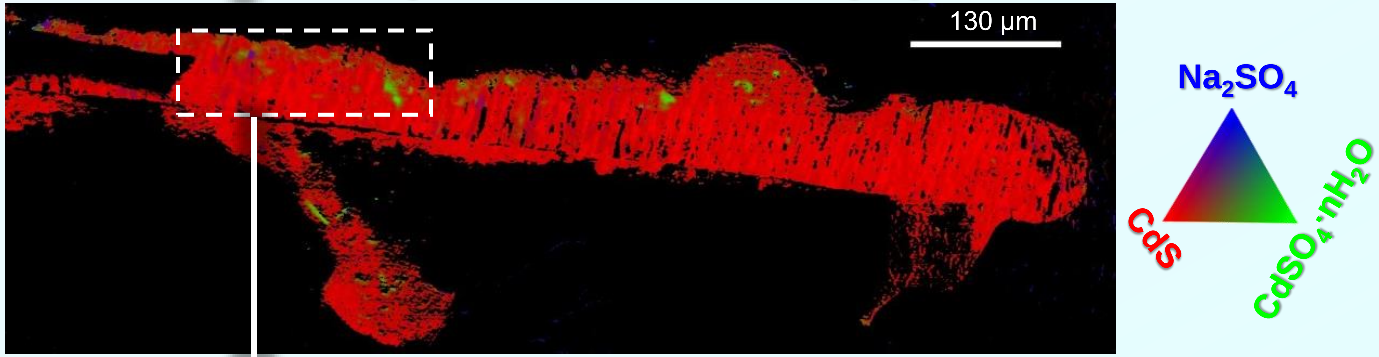

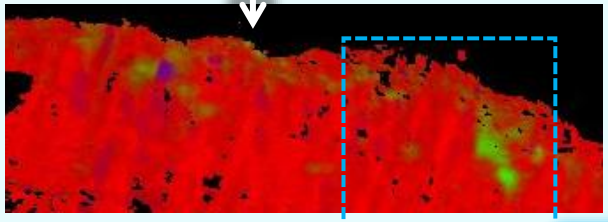

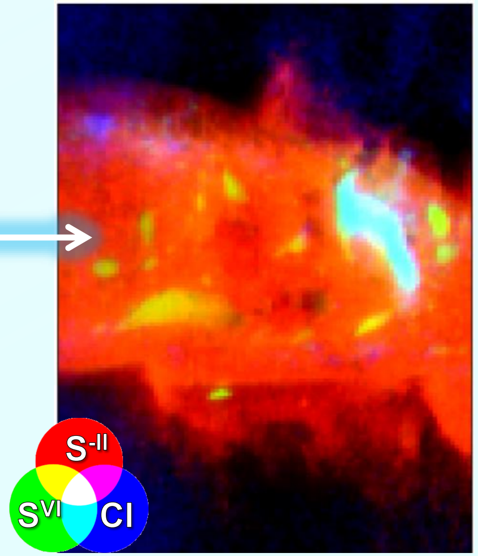

Co-localization of cadmium sulfate with Cl-compounds

Size map (h×v): 958.8x302.2 µm^2
Step size (h×v): 0.65×0.65 µm^2

MUNCH MUSEET

- High moisture conditions (RH≥95%) promote the formation of Cd/S^{VI} and Na/S^{VI} aggregates along with smaller amount of sulfites;
- Cl-compounds, originally homogenously distributed throughout the paint, become localized in the Cd/S^{VI} aggregates.

L. Monico *et al.*, *Science Advances* 6 (2020), eaay3514

3 - Alternative route of formation of $CdSO_4$

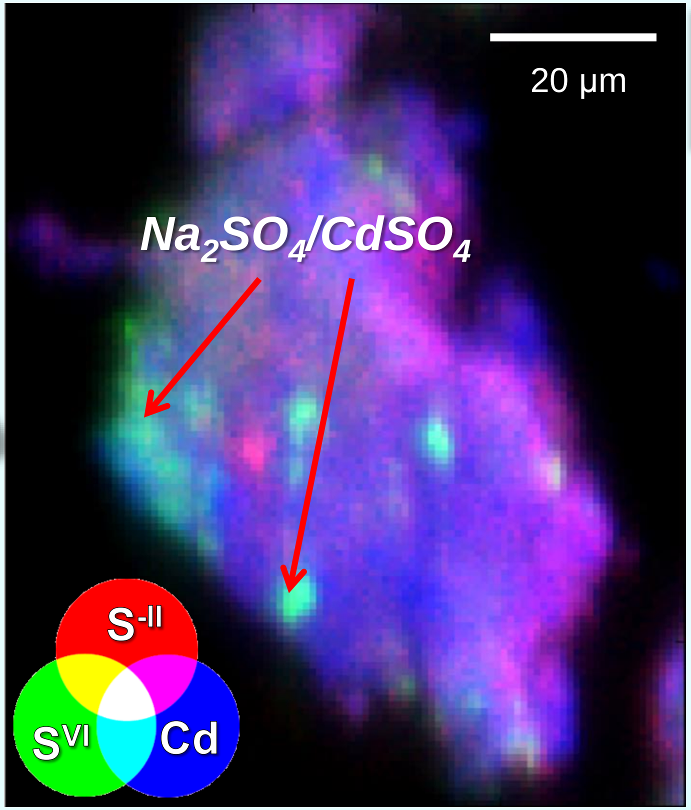

ESRF
ID21

Presence of Na_2SO_4 and other water soluble Cl-compounds (i.e., KCl, NaCl…) correlated to the starting reagents used for the synthesis of cadmium yellows

L. Monico *et al.*, *Science Advances* 6 (2020), eaay3514

3 - Alternative route of formation of $CdSO_4$

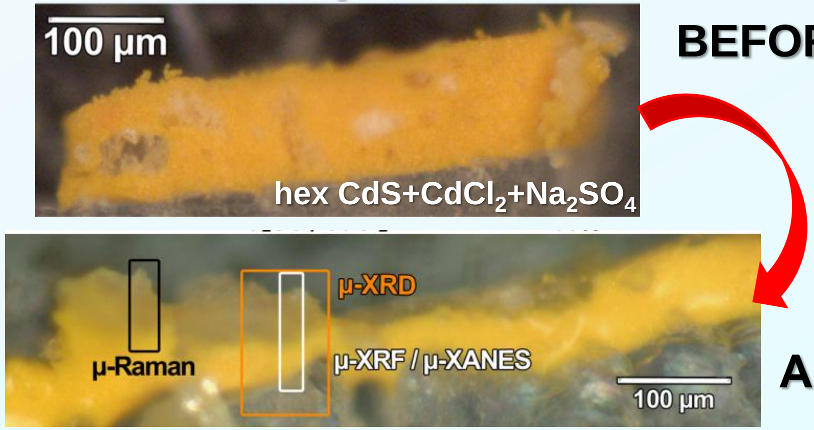

BEFORE

AFTER

- The formation of a "greyish crust" is visible after exposure to moisture.

μ-XRF/ μ-XANES

ESRF
ID21

μ-Raman

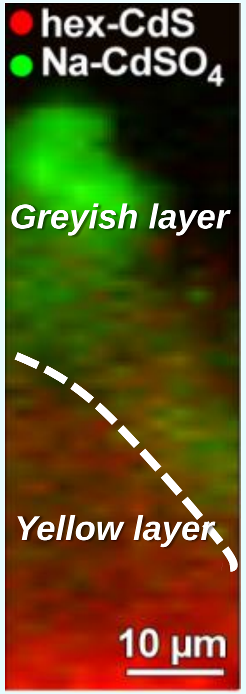

μ-XRD

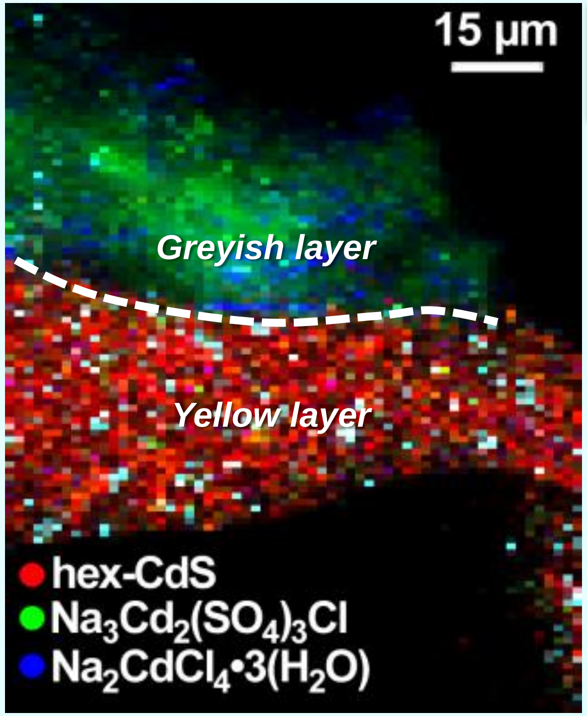

DESY
P06

- The reaction between Na_2SO_4 and $CdCl_2$ results in the formation of cadmium sulfate-based compounds.

L. Monico *et al.*, *Science Advances* 6 (2020), eaay3514

Darkening of chrome yellows

4- Darkening of chrome yellows ($PbCr_{1-x}S_xO_4$)*

➢ Characterized by low photochemical stability with tendency to lose their original brilliant yellow color.

Bank of the Seine (F293, mid May-late July 1887, Van Gogh Museum)

Falling leaves (Les Alyscamps) (F486, November 1888, Kröller-Müller Museum)

The bedroom (F482, October, 1888, Van Gogh Museum)

Sunflowers (F458, January 1889, Van Gogh Museum)

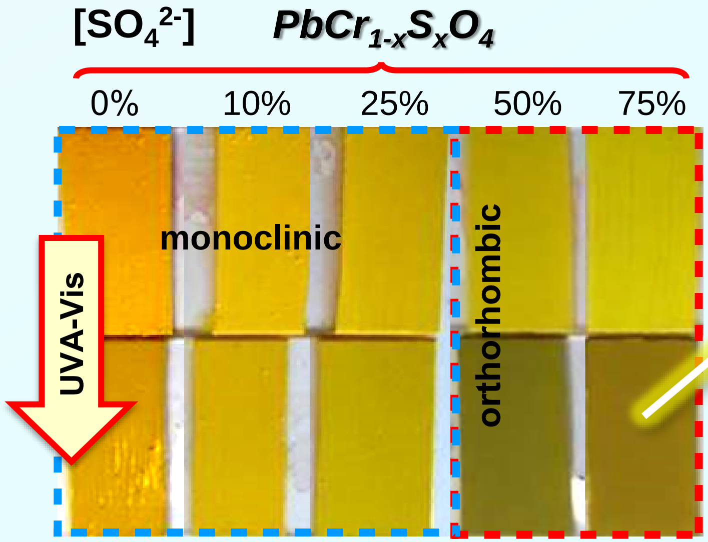

Photochemically aged paint mock-ups

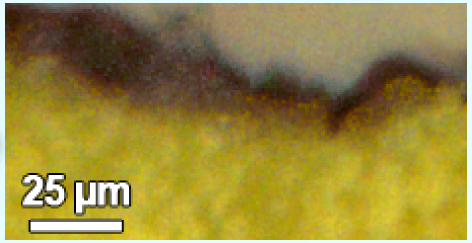

Thin alteration layer (thickness: <10 µm)

➢ ***Darkening due to a (photo)reduction process:***

$Cr^{VI} \rightarrow Cr^{III}$

➢ ***Cr-reduction depends on:***

a) Cr:S stoichiometry

b) Crystalline structure

c) Binding medium

d) Solubility of lead chromate-type

*L. Monico *et al., Anal. Chem.* 83 (2011) 1214–1223; L. Monico *et al., Anal. Chem.* 83 (2011) 1224-1231; L. Monico *et al., Anal. Chem.* 85 (2013) 860-867; L. Monico *et al., Anal. Chem.* 86 (2014) 10804–10811; L. Monico *et al., JAAS* 30 (2015) 613-626; L. Monico *et al., JAAS* 30 (2015) 1500-1510; L. Monico *et al., Angew. Chem. Int. Ed.* 54 (2015) 13923-13927; L. Monico *et al., ACS Omega* 4 (2019) 6607-6619.

4-Cr speciation investigations: Cr K-edge XANES

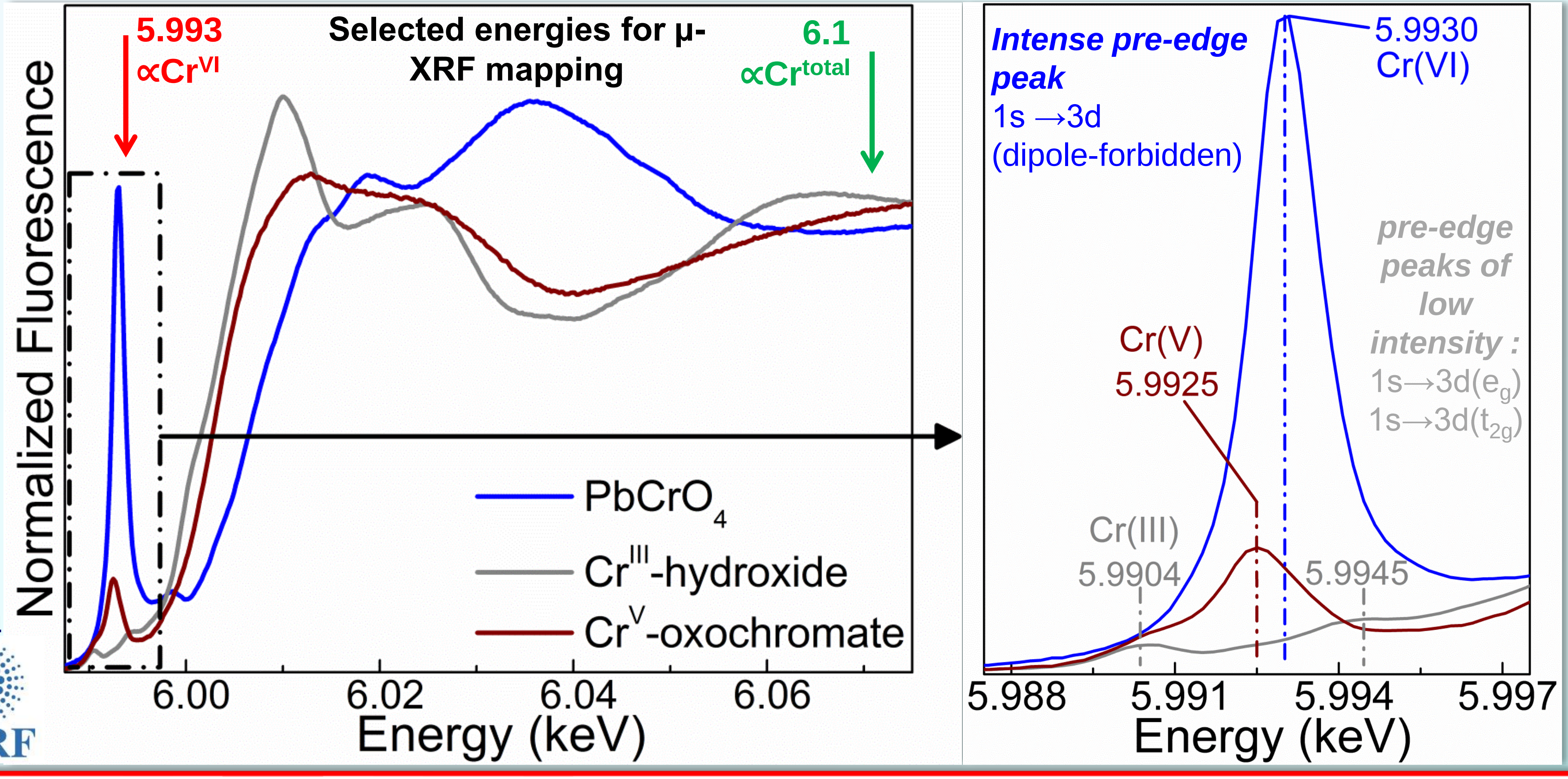

ID21 ESRF

- **Cr(VI) compounds:** non-centrosymmetric tetrahedral coordination.
- **Cr(III) compounds:** centrosymmetric octahedral geometry.
- Pre-edge peak area proportional to the relative amount of Cr(VI).
- Shift of the absorption edge position towards higher energies: ***increase of the valency*** of the absorbing atom and/or of the ***electronegativity*** of the nearest neighbour atoms.
- Identification of specific reduced Cr-compounds challenging, when different Cr-species are co-present.

Van Gogh Museum Amsterdam

CHARISMA

IPERION CH

4-Van Gogh’s Sunflowers (Amsterdam version)

Angewandte Chemie

Evidence for Degradation of the Chrome Yellows in Van Gogh’s *Sunflowers*: A Study Using Noninvasive In Situ Methods and Synchrotron-Radiation-Based X-ray Techniques

Letizia Monico, Koen Janssens, Ella Hendriks, Frederik Vanmeert, Geert Van der Snickt, Marine Cotte, Gerald Falkenberg, Brunetto Giovanni Brunetti, and Costanza Miliani*

Angew. Chem. **2015**, 127, 14129–14133

Chemical Mapping by Macroscopic X-ray Powder Diffraction (MA-XRPD) of Van Gogh’s *Sunflowers*: Identification of Areas with Higher Degradation Risk

Frederik Vanmeert, Ella Hendriks, Geert Van der Snickt, Letizia Monico, Joris Dik, and Koen Janssens*

Angew. Chem. Int. Ed. **2018**, 57, 7418–7422

Amsterdam University Press

2019

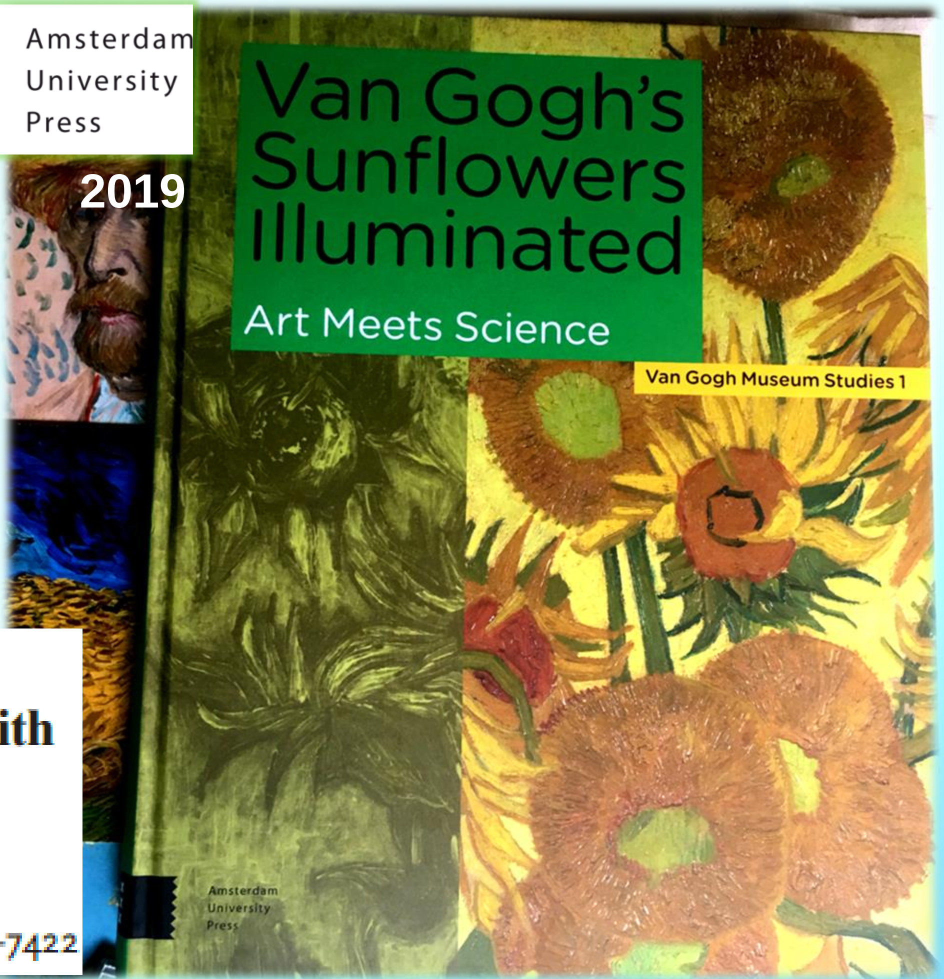

4-Cr speciation analyses: aged paint mock-ups & historical paint micro-samples*

$PbCr_{0.2}S_{0.8}O_4$

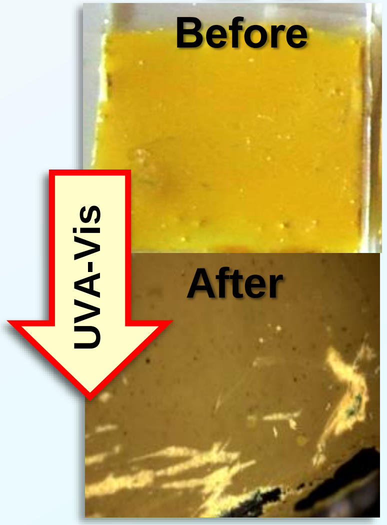

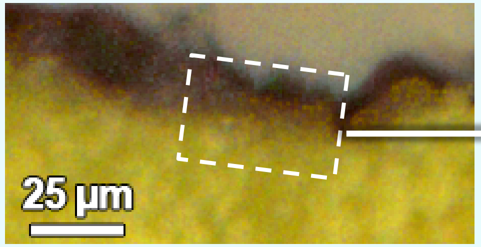

Thin section
(thickness: ~5 µm)

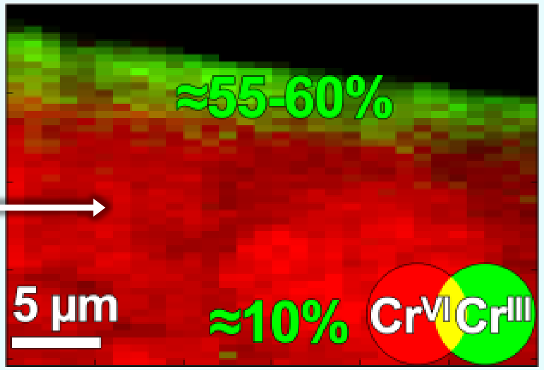

step size (h×v): 0.8×0.3 µm^2
dwell time: 100 ms/pixel
Energy: 5.993-6.1 keV

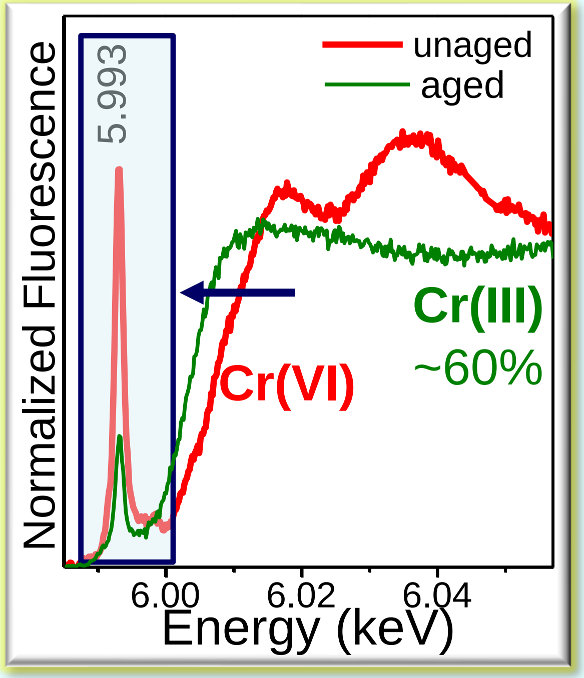

ID21
ESRF

Sunflowers (F458, January 1889, Van Gogh Museum)

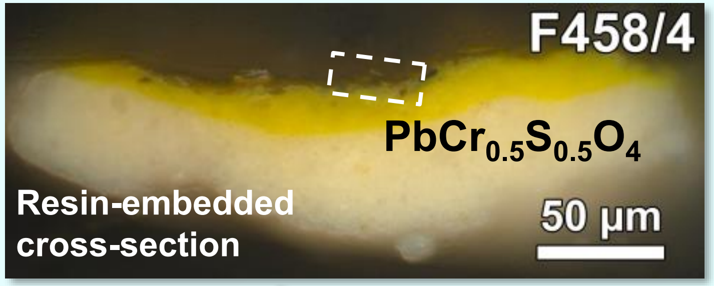

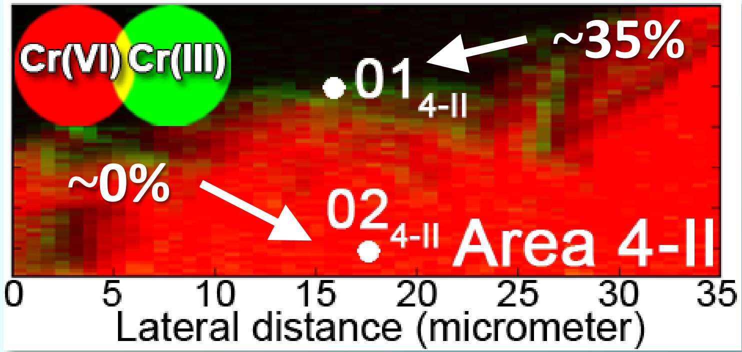

step size (h×v): 0.7×0.2 µm^2
dwell time: 100 ms/pixel
Energy: 5.993-6.1 keV

*L. Monico *et al.*, *Anal. Chem.* 85 (2013) 860-867; L. Monico *et al.*, *JAAS* 30 (2015) 1500-1510;
L. Monico *et al.*, *Angew. Chem. Int. Ed.* 54 (2015) 13923-13927.

4-Maia and SDD-detector based microprobe systems: The Bedroom*

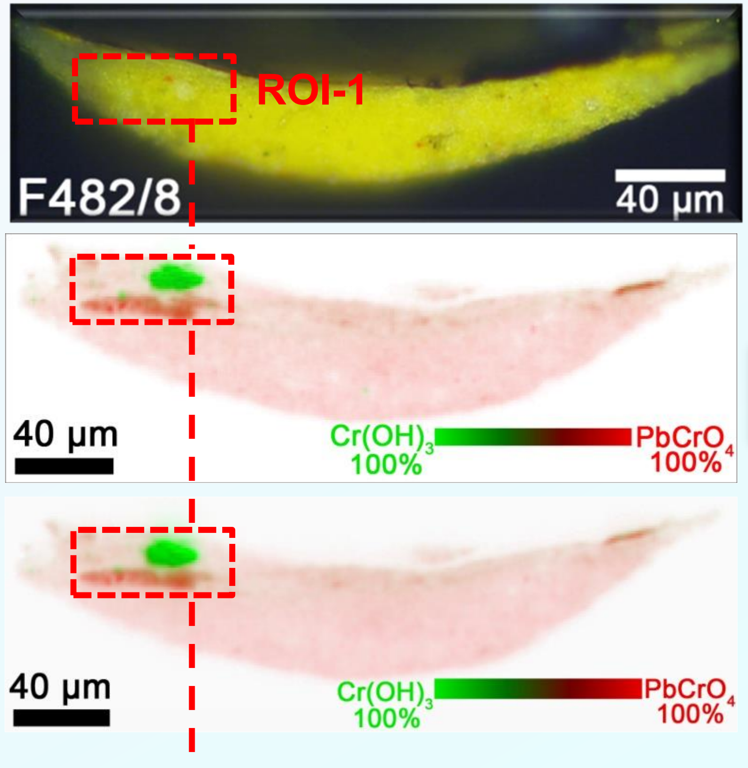

Maia-XFM

Australian Synchrotron

Maia-P06

SDD-ID21

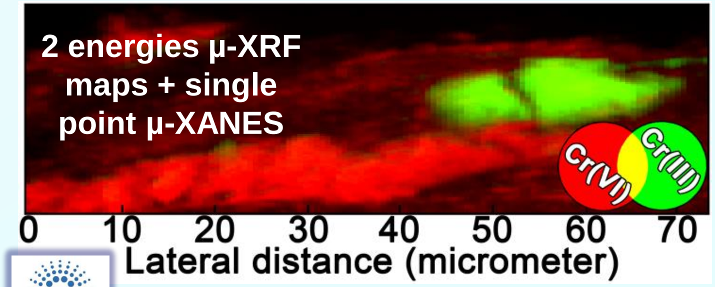

The Bedroom (V. van Gogh, October 1888, Van Gogh Museum, Amsterdam).

↑ Faster acquisition time (factor of 10^2 -10^3 shorter per energy scan)
↑ More representative datasets (analysis of larger areas- larger n. of XANES spectra)
↑ Lower fluences (2-3 order of magnitude; decreasing of beam damage probability)

↓ Lower spatial/lateral resolution (~0.7-2 µm)
↓ Lower spectral energy resolution
↓ Stage platform less stable (Y drift correction /re-alignment)
↓ Lower fluences (lower signal to noise ratio)

Microprobe system	Map size (h×v) (µ²)	Pixel size (h×v) (µm²)	Pixel total number	Dwell time (ms/pixel)	Acquisition time (min)	Absolute photon flux (ph/s)	fluence (ph/µm²)
Maia-P06	300×80	1×1	2.4×10^4	3	210	9×10^8	8×10^8
Maia-XFM	300×80	1×1	2.4×10^4	0.99	130	2.1×10^8	2.6×10^7
SDD-ID21	73.8×22.6	0.6×0.2	1.3899×10^4	150-300	108	1.7×10^8	3.3×10^7

* L. Monico *et al.*, *JAAS* 30 (2015) 613-626.

4-Cr K-edge full field-XANES imaging of chromate-based yellows

➢ ***FF-XANES imaging of chrome yellow samples?***

Challenging/not possible due to the matrix composition ($PbCr_{1-x}S_xO_4$):

- presence of Pb
- Cr concentration

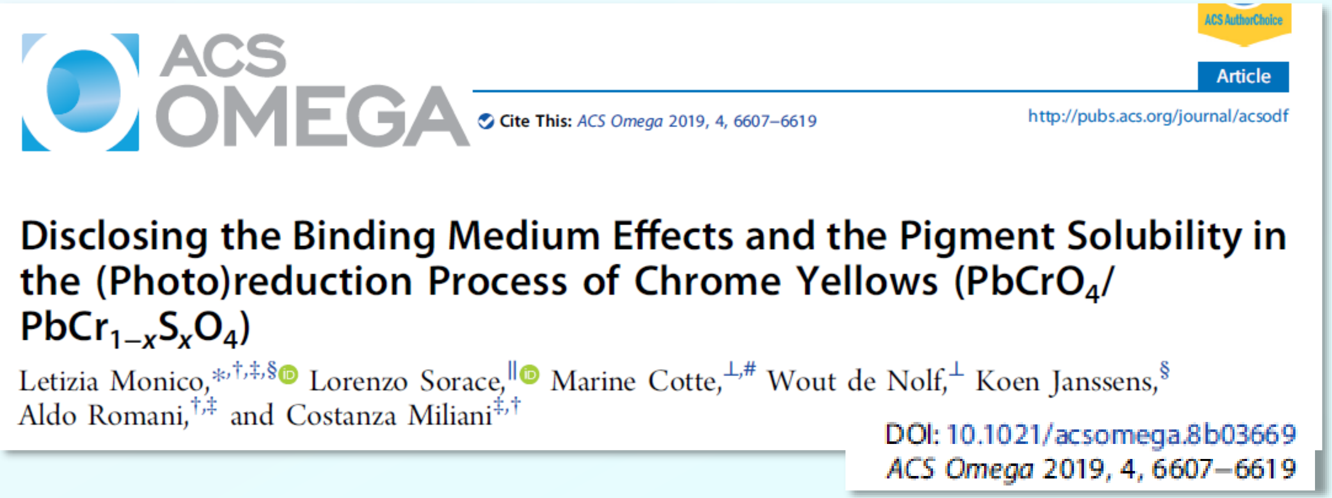

ACS OMEGA

ACS AuthorChoice

Article

Cite This: *ACS Omega* 2019, 4, 6607−6619

http://pubs.acs.org/journal/acsodf

Disclosing the Binding Medium Effects and the Pigment Solubility in the (Photo)reduction Process of Chrome Yellows ($PbCrO_4$/$PbCr_{1-x}S_xO_4$)

Letizia Monico,[*,†,‡,§] Lorenzo Sorace,[∥] Marine Cotte,[⊥,#] Wout de Nolf,[⊥] Koen Janssens,[§] Aldo Romani,[†,‡] and Costanza Miliani[‡,†]

DOI: 10.1021/acsomega.8b03669

ACS Omega 2019, 4, 6607−6619

the different stability of different chrome yellow types is related to their different solubility

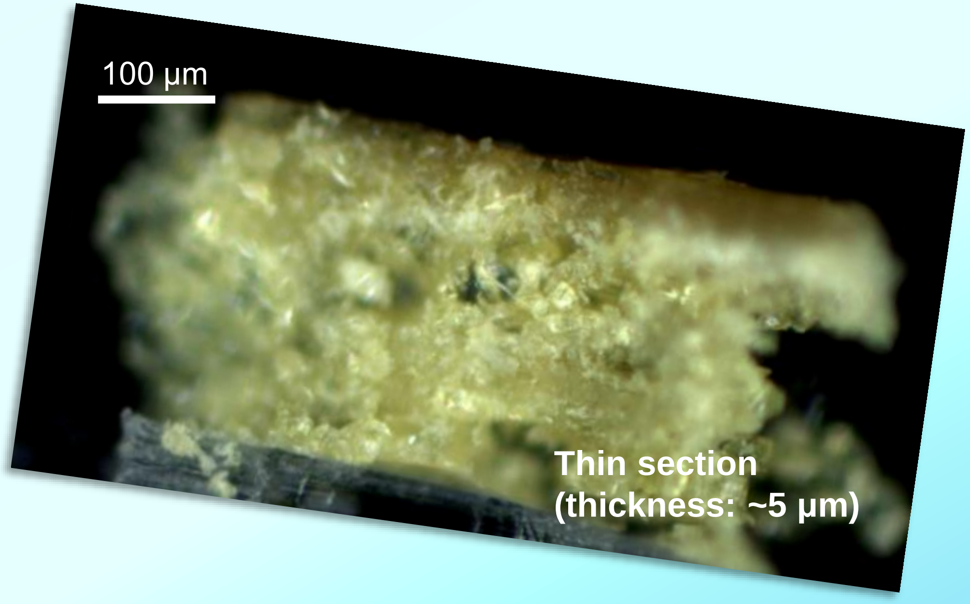

K_2CrO_4 Powder (without binder)

K_2CrO_4+linseed oil
(naturally aged for 4 months)

Situation very similar to the most altered light-sensitive chrome yellow pigments

4-Cr K-edge full field-XANES imaging of chromate-based yellows

FF-XANES imaging

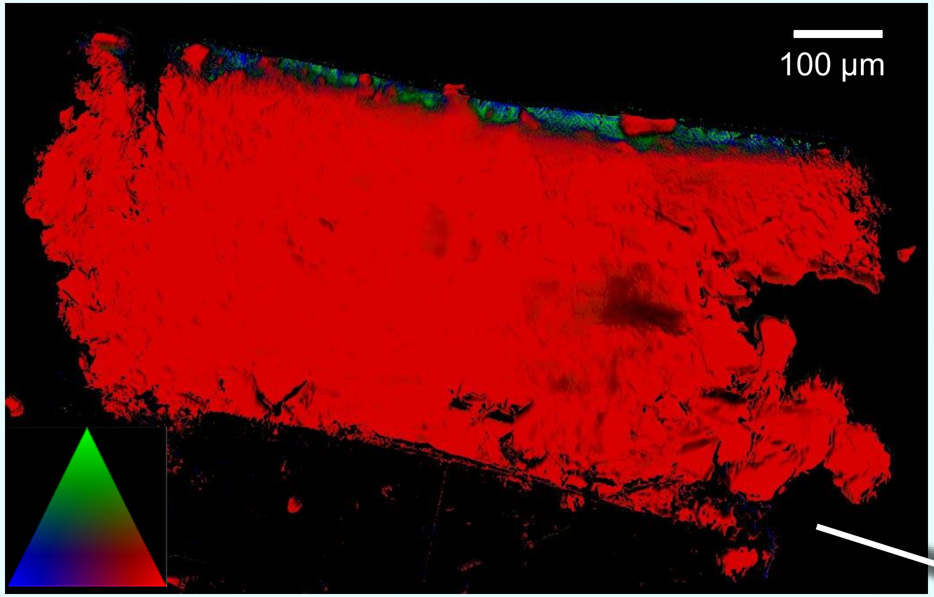

K_2CrO_4

Cr^{III}-hydroxide/organo Cr^{III}-compounds

Cr^{V}-oxochromate

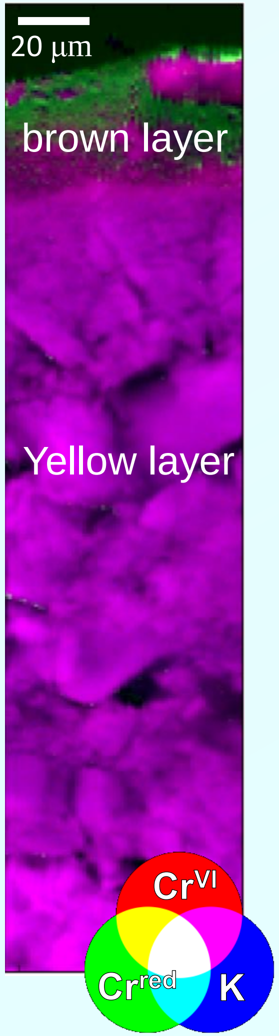

2 energies µ-XRF maps + single point µ-XANES

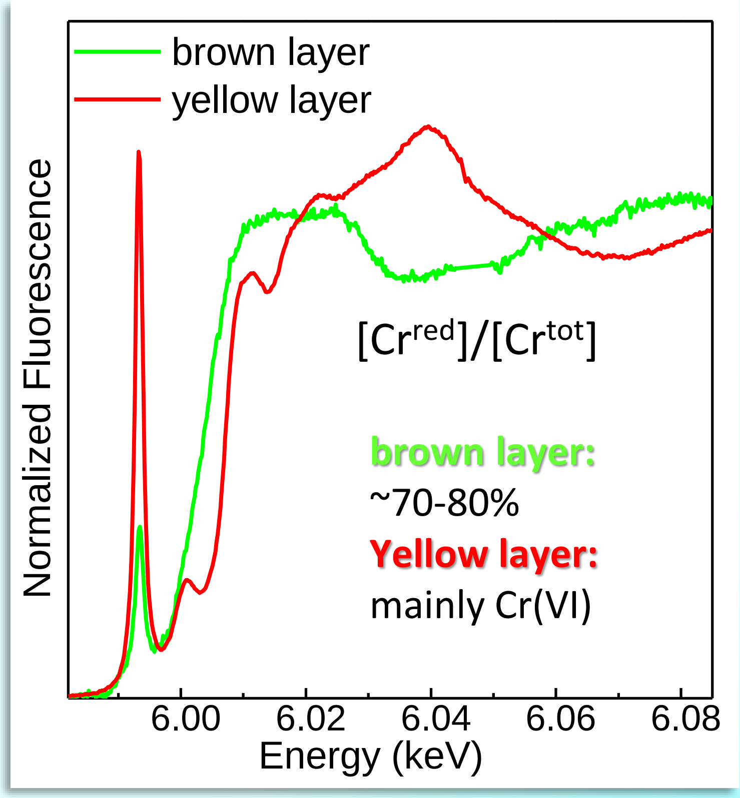

- No limitations due to the matrix composition;

- FF-XANES imaging of other chromate-based yellows [e.g. zinc yellow: $KZn_2(CrO_4)_2(H_2O)(OH)$].

L. Monico *et al.*, *ACS Omega* 4 (2019) 6607-6619.

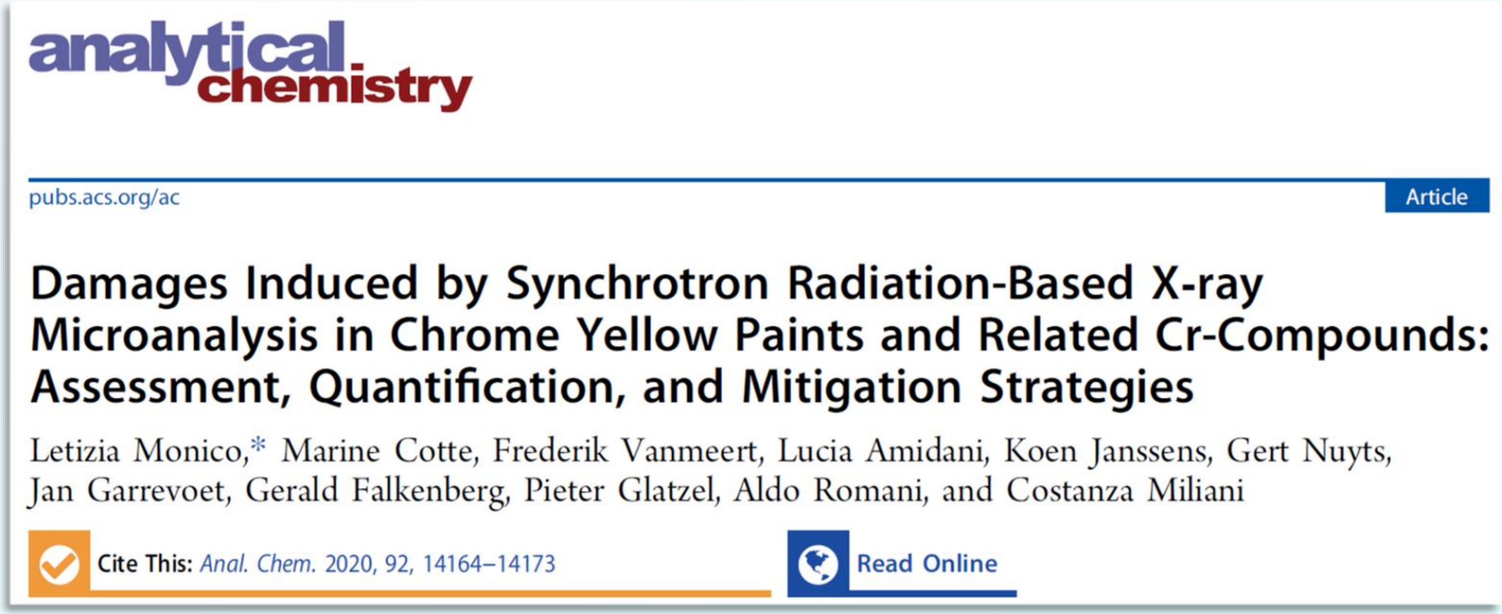
analytical chemistry

pubs.acs.org/ac | Article

Damages Induced by Synchrotron Radiation-Based X-ray Microanalysis in Chrome Yellow Paints and Related Cr-Compounds: Assessment, Quantification, and Mitigation Strategies

Letizia Monico,* Marine Cotte, Frederik Vanmeert, Lucia Amidani, Koen Janssens, Gert Nuyts, Jan Garrevoet, Gerald Falkenberg, Pieter Glatzel, Aldo Romani, and Costanza Miliani

Cite This: *Anal. Chem.* 2020, 92, 14164–14173 | Read Online

- ***ID26:*** *Cr-K_β XES/ Cr K-edge high-energy resolution fluorescence detected (HERFD)-XANES*
- ***ID21:*** *μ-XRF/Cr K-edge μ-XANES*
- ***P06:*** *μ-XRD*

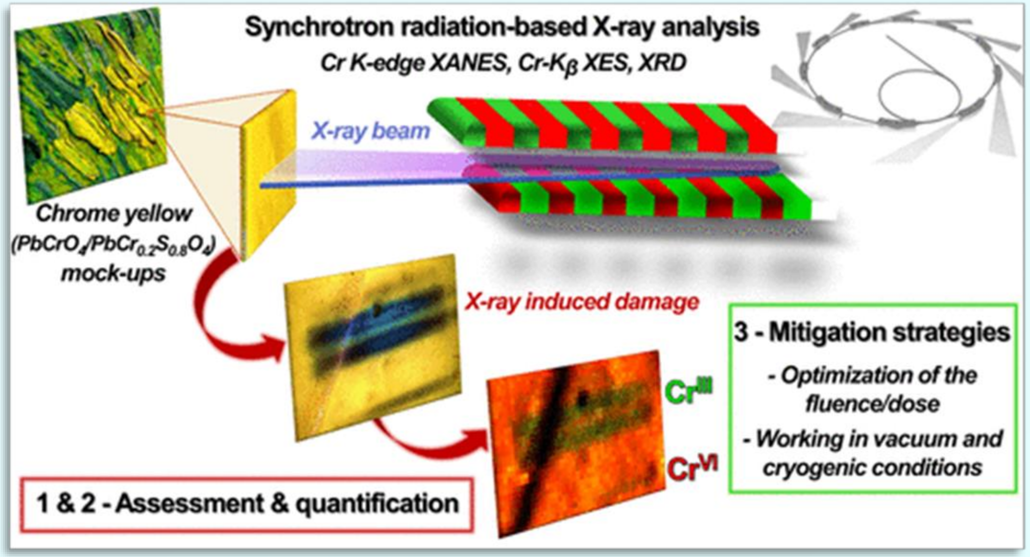

light-fast $PbCrO_4$

oil *acrylic*

powder

light-sensitive $PbCr_{0.2}S_{0.8}O_4$

oil *acrylic*

powder

4- Cr-K_{β} XES/ Cr K-edge HERFD-XANES (ID26)

ID26

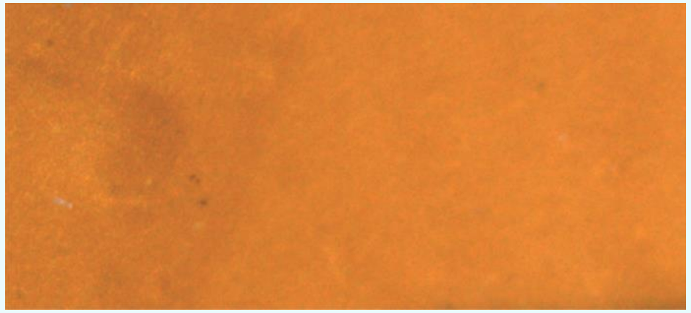

$PbCrO_4$-oil

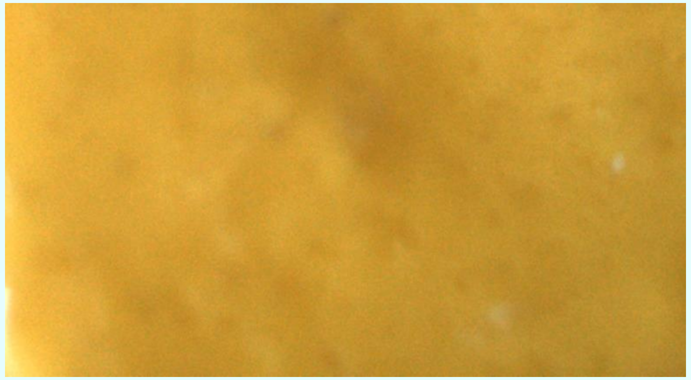

$PbCr_{0.2}S_{0.8}O_4$-oil

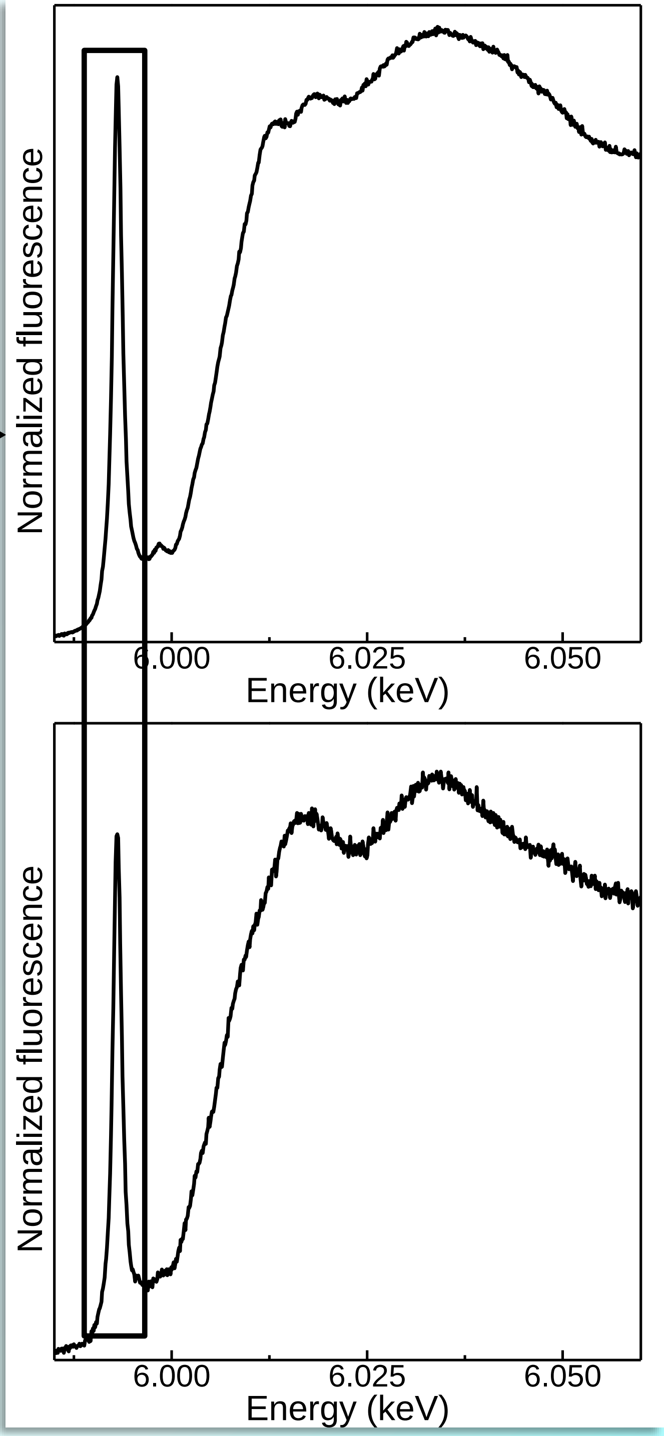

***Before Cr Kβ XES*:**
Cr^{VI}-species

L. Monico *et al.*, *Anal. Chem.* 92 (2020) 14164-14173.

4- Cr-K$_\beta$ XES/ Cr K-edge HERFD-XANES (ID26)

ESRF

ID26

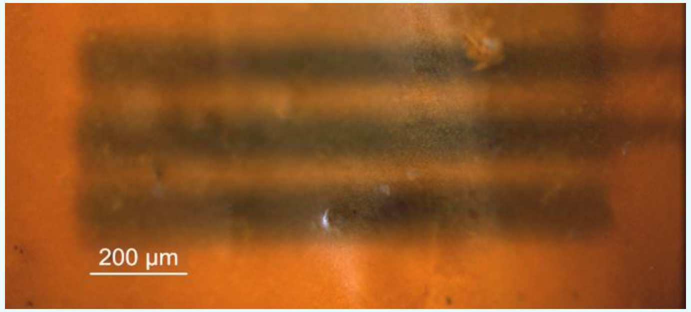

$PbCrO_4$-oil

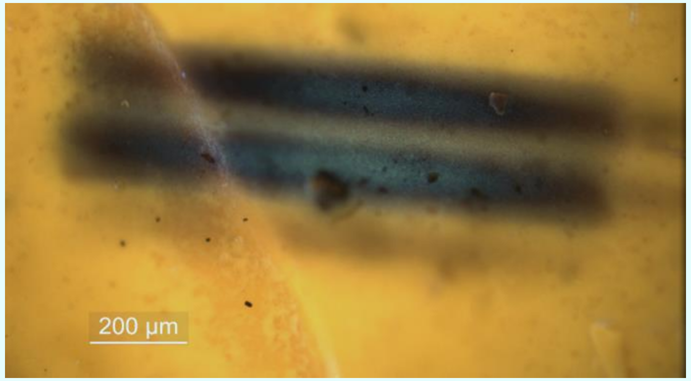

$PbCr_{0.2}S_{0.8}O_4$-oil

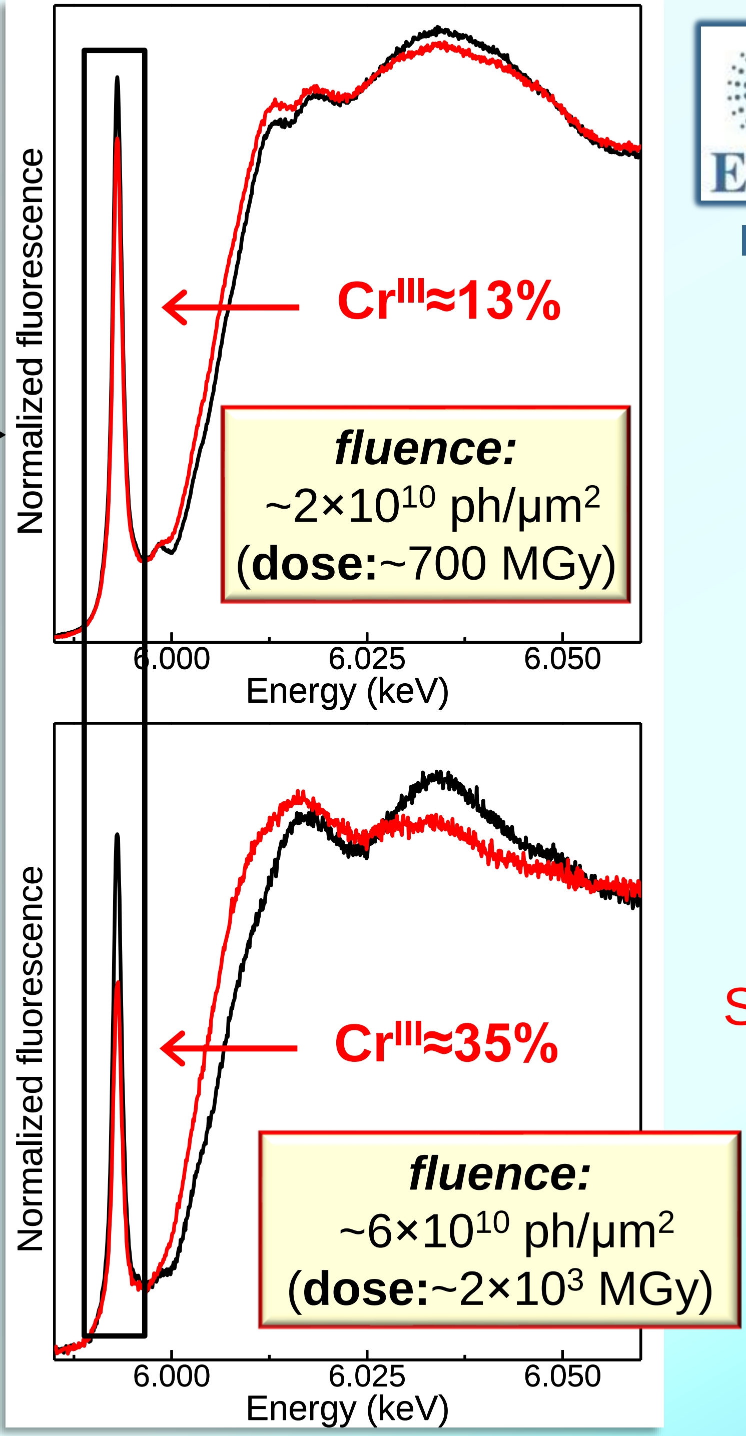

***Before Cr Kβ XES*:**
Cr^{VI}-species

***After Cr Kβ XES*:**
SR X-ray induced reduction process

L. Monico *et al.*, *Anal. Chem.* 92 (2020) 14164-14173.

4-Cr-speciation mapping (ID21)

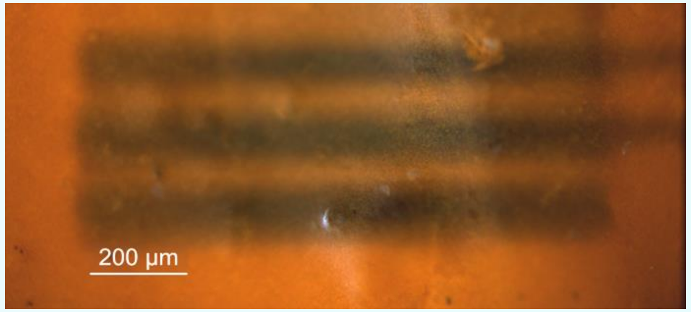

PbCrO$_4$-oil

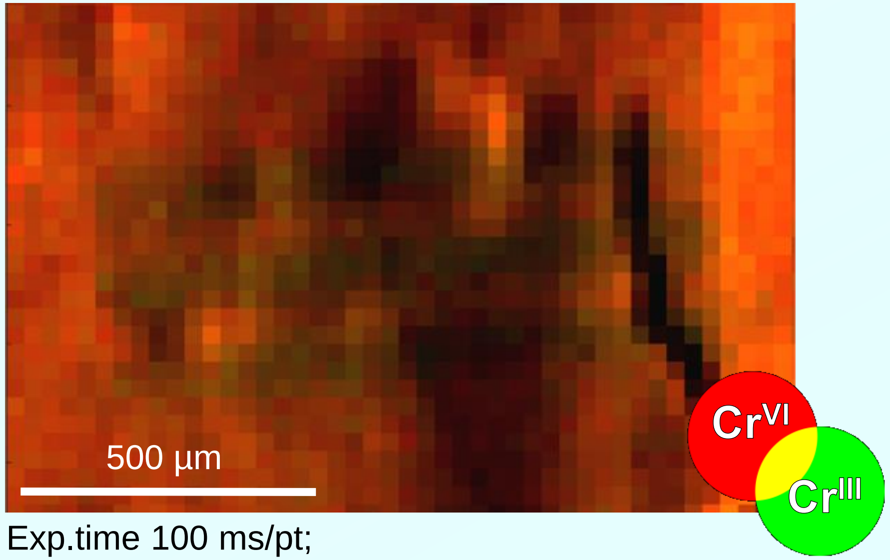

Exp.time 100 ms/pt;
Size (h×v):1.5×1.2 mm^2
Step: 30×30 µm^2

"Burnt" areas: Cr-reduction

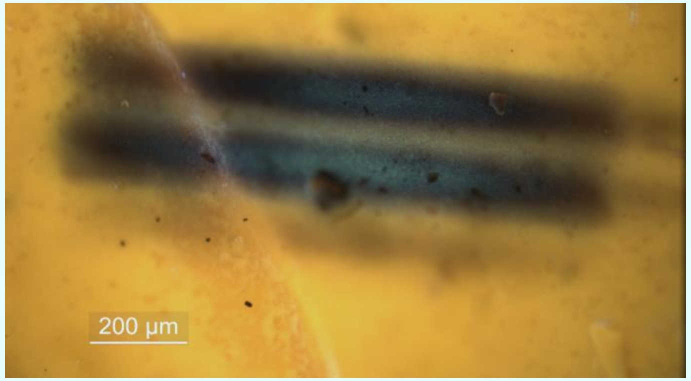

PbCr$_{0.2}$S$_{0.8}$O$_4$-oil

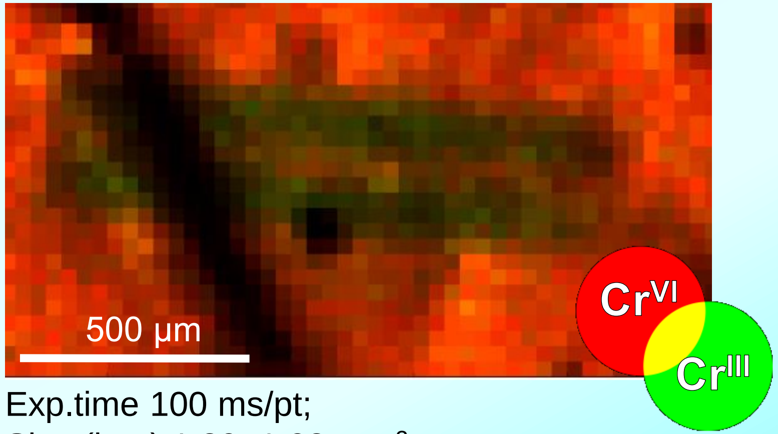

Exp.time 100 ms/pt;
Size (h×v):1.89×1.08 mm^2
Step: 30×30 µm^2

ID21

L. Monico *et al.*, *Anal. Chem.* 92 (2020) 14164-14173.

4-Cr K-edge µ-XANES (ID21): effect of Cr:S stoichiometry

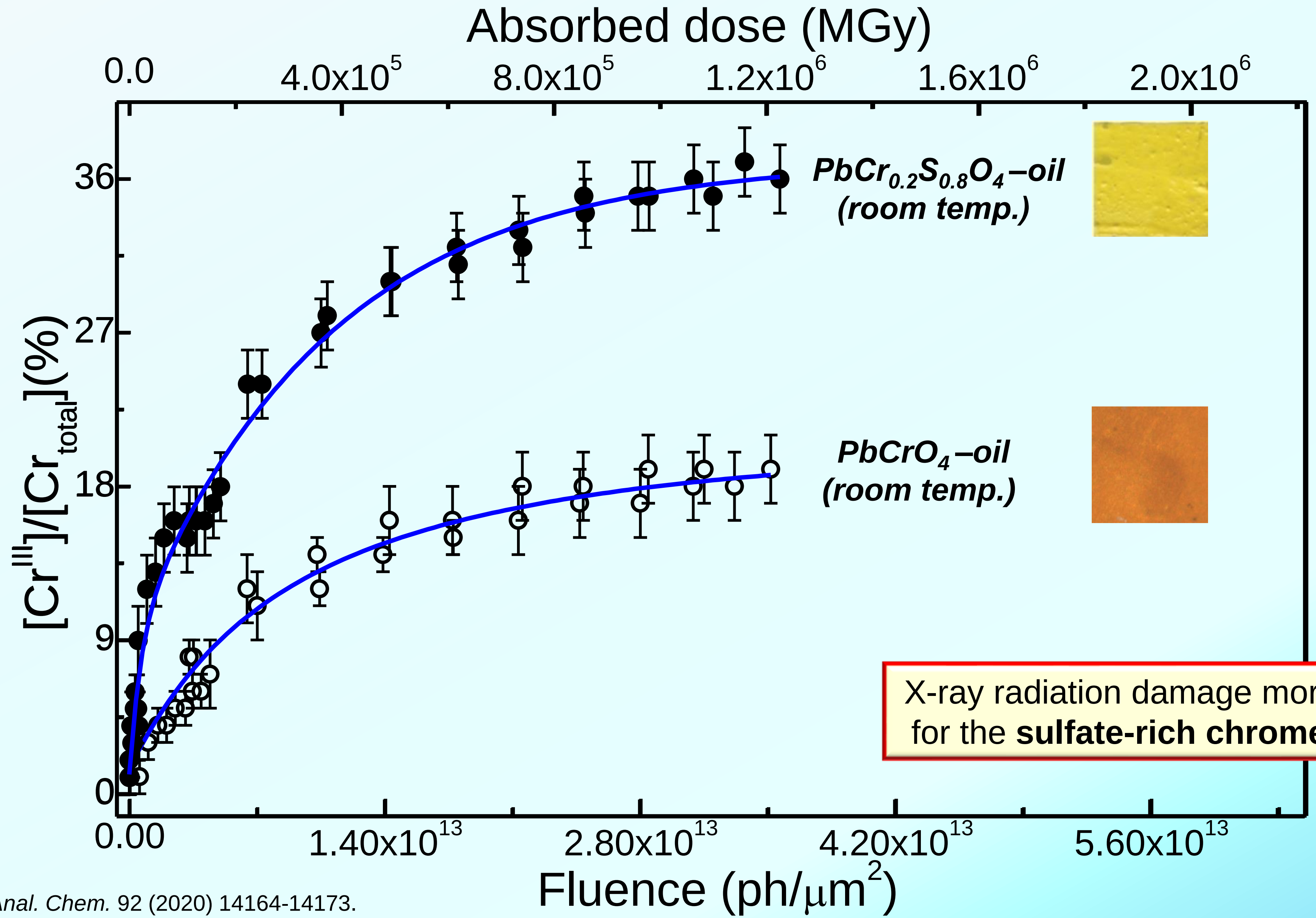

ID21

ESRF

X-ray radiation damage more pronounced for the **sulfate-rich chrome yellow type**

L. Monico *et al.*, *Anal. Chem.* 92 (2020) 14164-14173.

4-Cr K-edge µ-XANES (ID21): effect of the binding medium

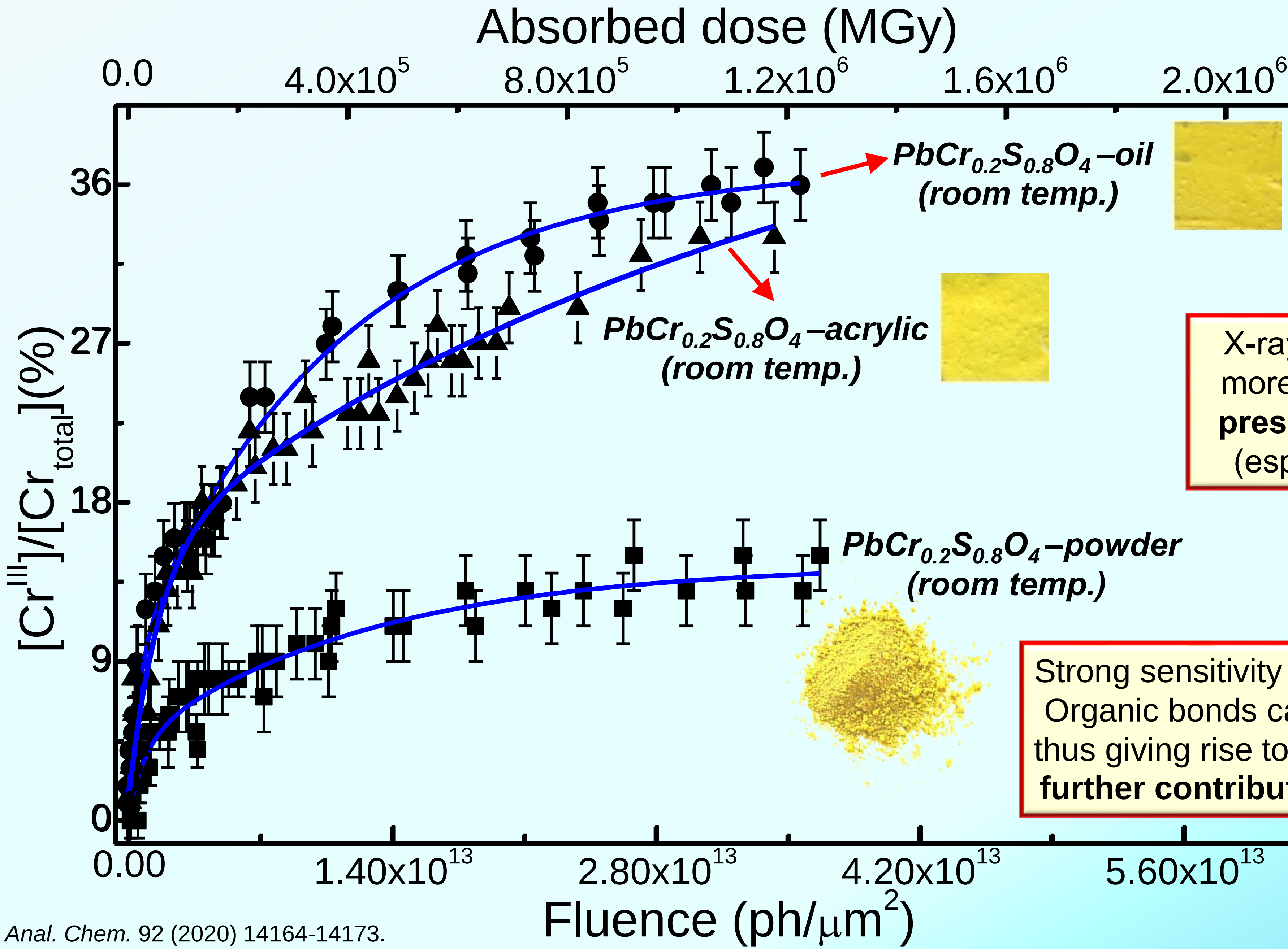

ID21 ESRF

X-ray radiation damage more pronounced in the **presence of the binder** (especially linseed oil)

Strong sensitivity of organic materials. Organic bonds can be easily broken, thus giving rise to **radicals**, which can **further contribute to Cr^{VI}-reduction**

L. Monico *et al.*, *Anal. Chem.* 92 (2020) 14164-14173.

4- μ-XRD (P06-PETRA III)

$PbCrO_4$–oil ***$PbCr_{0.2}S_{0.8}O_4$–oil***

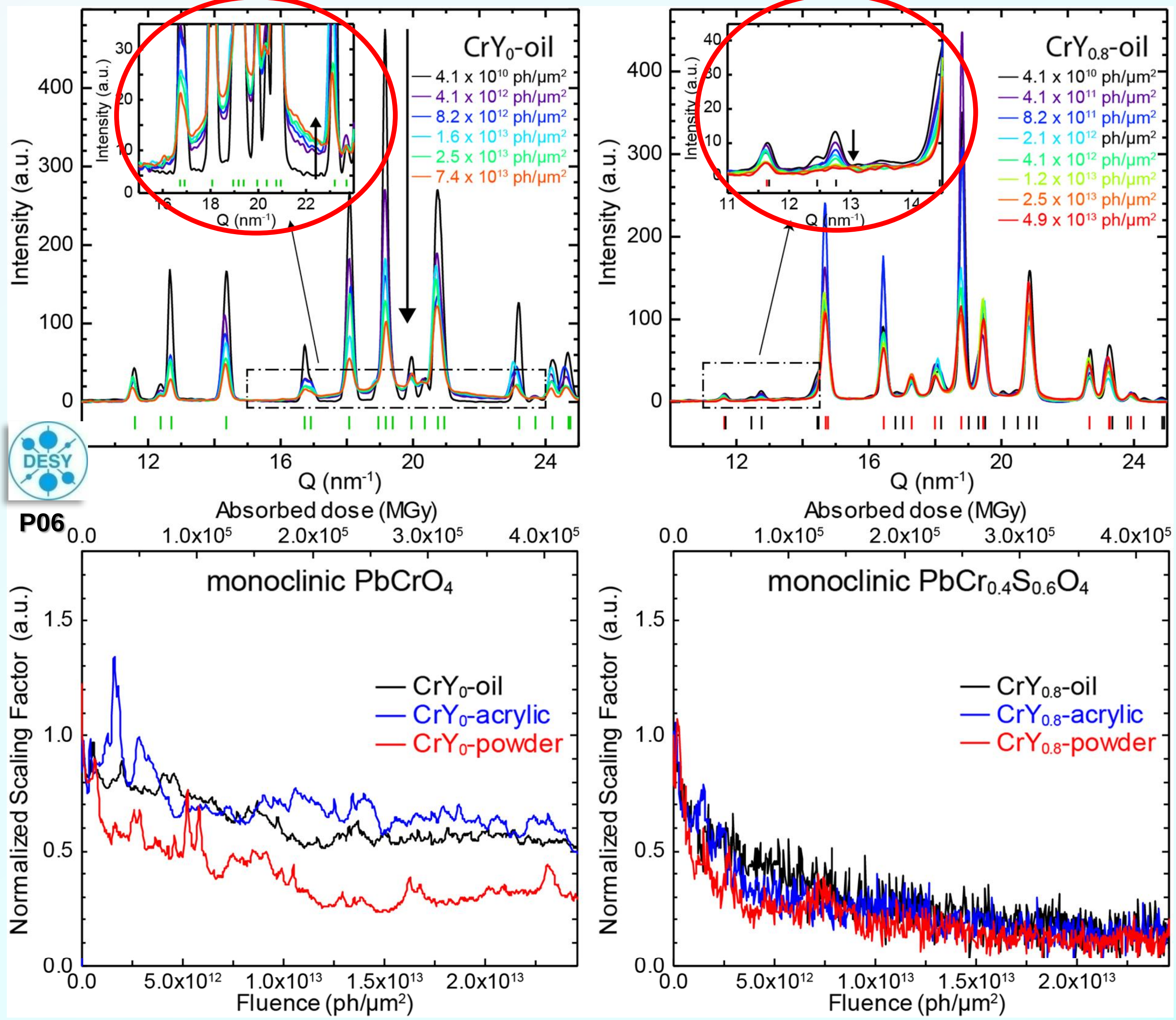

> ➢ Formation of an amorphous phase (clearly visible for $PbCrO_4$–oil).
> ➢ Loss of crystalline structure (decreasing of the intensity of the diffraction signals);
> ➢ It is more pronounced for the sulfate-richer phases;

Cr-speciation mapping

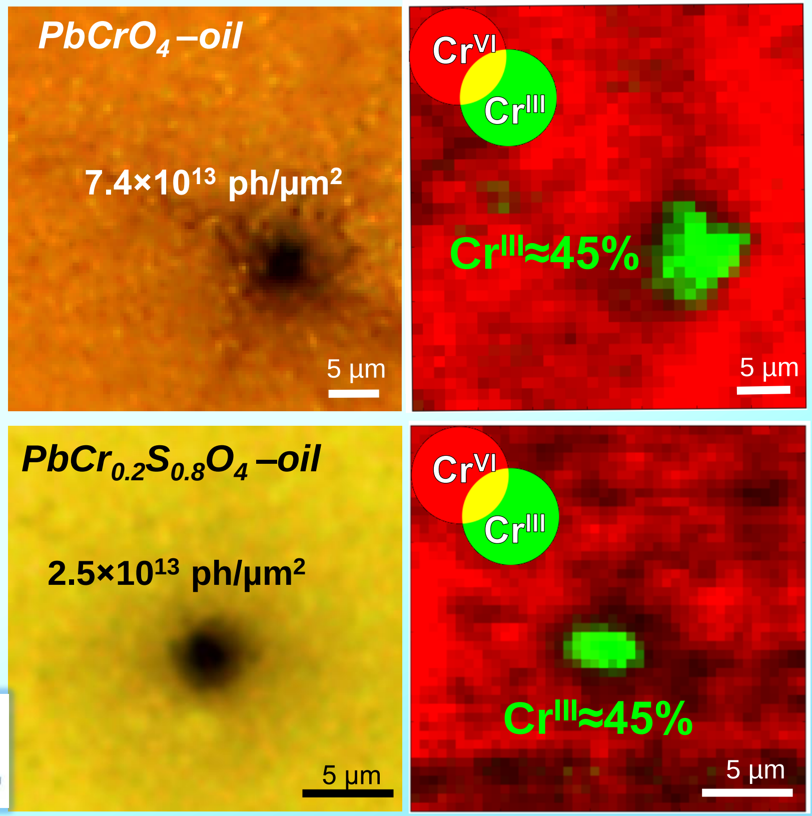

L. Monico *et al.*, *Anal. Chem.* 92 (2020) 14164-14173.

4-Mitigation strategies: optimization of the fluence/dose

- Assessment of the **fluence/dose threshold** at which X-rays start to induce spectral changes in the data;

Beamline	Energy (keV)	Fluence threshold (ph/μm^2)	Absorbed dose threshold (MGy)
ESRF-ID21	~6	~5×10^{11}	~2×10^{4}
ESRF-ID26	~6	~10^{8}	~10
DESY-P06	21	~$1\text{-}2\times10^{11}$	~$2\text{-}4\times10^{3}$

- **Adapt time** to stay below the established threshold value (fast-data acquisition – ID26 beamline);

- **Decreasing the flux** of the incoming beam (e.g., using attenuators of different thickness) as long as an adequate signal-to-noise-ratio is maintained;

- **Defocusing the beam** to minimize the fluence/dose to the sample, but sometimes at the expense of spectral resolution (e.g., XES analysis).

L. Monico *et al.*, *Anal. Chem.* 92 (2020) 14164-14173.

4-Mitigation strategies: measuring under vacuum conditions

- **Different extent** of **photo-induced reduction** for **similar doses** (different fluence/dose threshold);

Beamline	Energy (keV)	Fluence threshold (ph/µm^2)	Absorbed dose threshold (MGy)	Vacuum
ESRF-ID21	~6	~5×10^{11}	~2×10^{4}	Yes
ESRF-ID26	~6	~10^{8}	~10	No
DESY-P06	21	~$1\text{-}2\times10^{11}$	~$2\text{-}4\times10^{3}$	No

- **vacuum conditions:** can explain the lower Cr^{III}-abundances obtained at ESRF-ID21;

- such sample environment may contribute to **indirectly slowing down Cr-reduction** due to the **absence/neglectable content of air gases (e.g., O_2) and moisture,** which favor the oxidative degradation of the binder.

L. Monico *et al.*, *Anal. Chem.* 92 (2020) 14164-14173.

4-Mitigation strategies: lowering the temperature

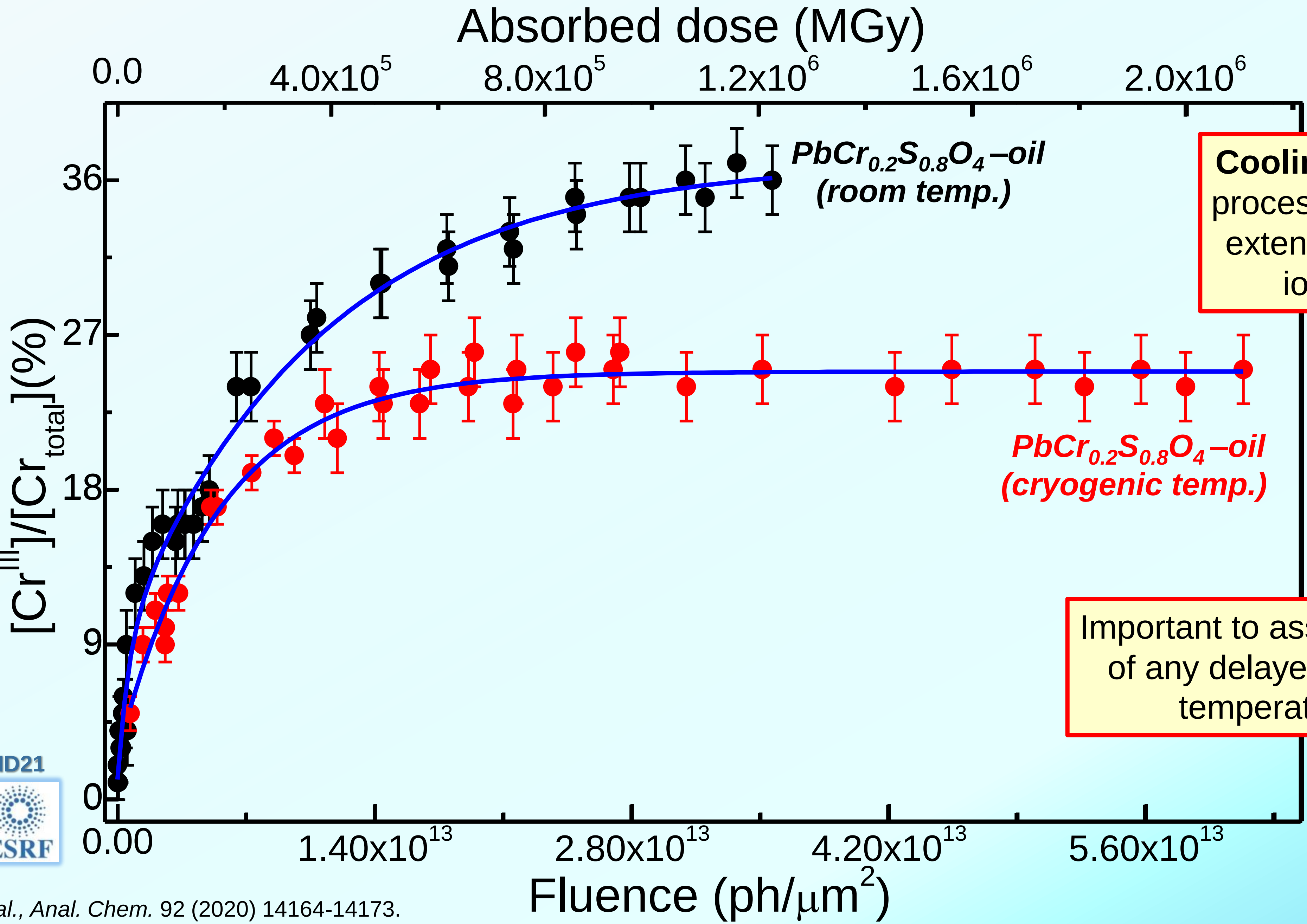

Cooling reduces diffusive processes and hinders the extensive propagation of ions and radicals

Important to assess the occurrence of any delayed damages due to temperature changes.

ID21

ESRF

L. Monico *et al.*, *Anal. Chem.* 92 (2020) 14164-14173.

Fading of Prussian blue

5-Prussian blue (PB) fading in Danish Golden Age paintings (19th c.)

CATS Centre for Art Technological Studies and Conservation

SMK Statens Museum for Kunst National Gallery of Denmark

- **PB:** mixed valence transition metal compound characterized by hydrated iron(III) hexacyanoferrate(II) complexes [***$Fe_4^{III}[Fe^{II}(CN)_6]_3 \cdot xH_2O$ or $MFe^{III}[Fe^{II}(CN)_6] \cdot xH_2O$, M: K^+, NH_4^+, Na^+];***
- intense blue coloration due to an intervalence charge transfer between the Fe(II) and Fe(III) ions bridged by the CN^- ligand.
- fading due to a photo-redox process that breaks the electron transfer Fe^{II}–CN–Fe^{III} pathway.[b]

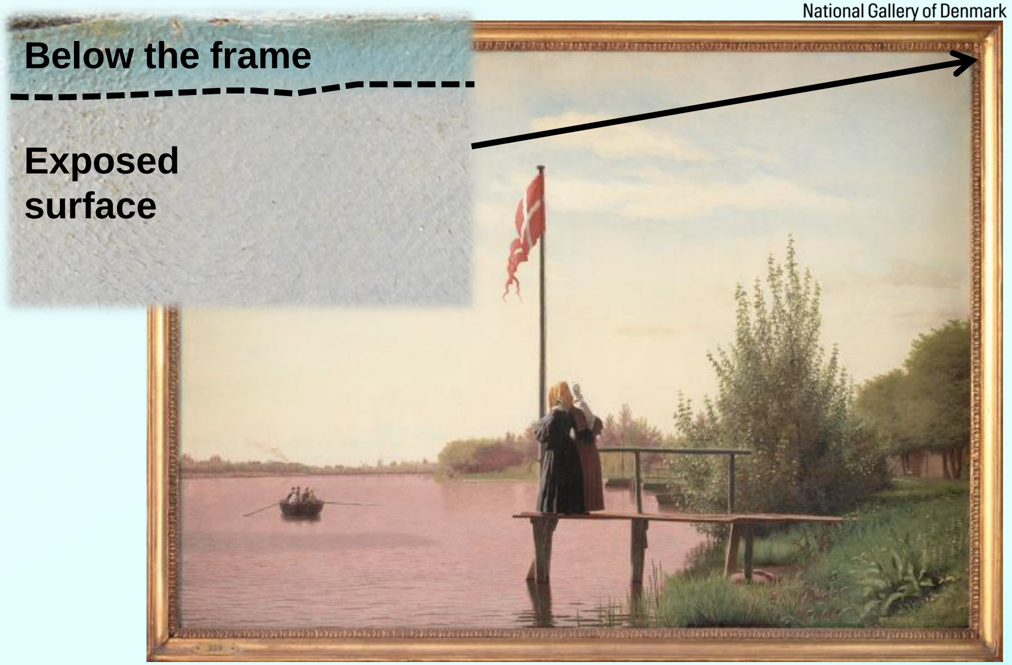

View of Lake Sortedam from Dosseringen Looking Towards the Suburb Nørrebro outside Copenhagen (1838, C. Købke; SMK, Copenhagen, DK).[a],[f]

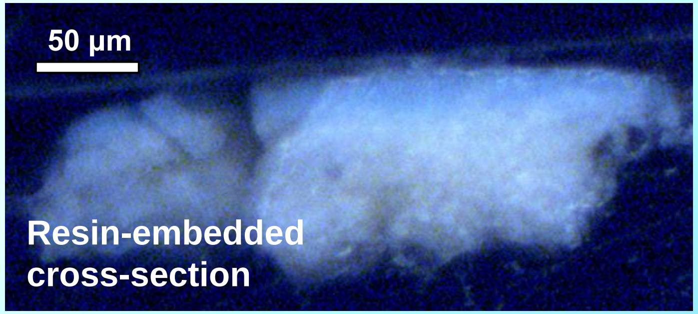

- Research question:

Is the fading due to **$Fe^{III} \rightarrow Fe^{II}$ reduction?**

- Experimental challenges:

a) PB is sensitive towards the exposure to X-ray microprobes;[c-e]

b) pigment diluted (low Fe concentration) in a lead white-rich matrix (FF-XANES imaging challenging/not possible)

[a] A. Vila *et al.*, in: "Science and Art: The Painted Surface" (Eds: A. Sgamellotti, B. G. Brunetti, C. Miliani), RSC, London, 2014, pp. 354-372; [b] L. Samain *et al.*, *JAAS* 26 (2011) 930–941 and 28 (2013) 524–535; [c] C. Gervais *et al.*, *JAAS* 28 (2013) 1600-1609; [d] C. Gervais *et al.*, *Langmuir* 31 (2015) 8168-8175; [e] C. Gervais *et al.*, *Appl. Physics A* 121 (2015) 949-955; [f] D. Buti *et al.*, Probing the fading of Prussian blue: from the macro non-invasive approach to the micro SR-based analysis. In *Gordon Research Conference: Scientific Methods in Cultural Heritage Research* (2018).

5- Assessment of the photostability of PB : Fe K-edge XANES

Unfocused mode-flux: 1×10^{9}-1×10^{10} ph/s

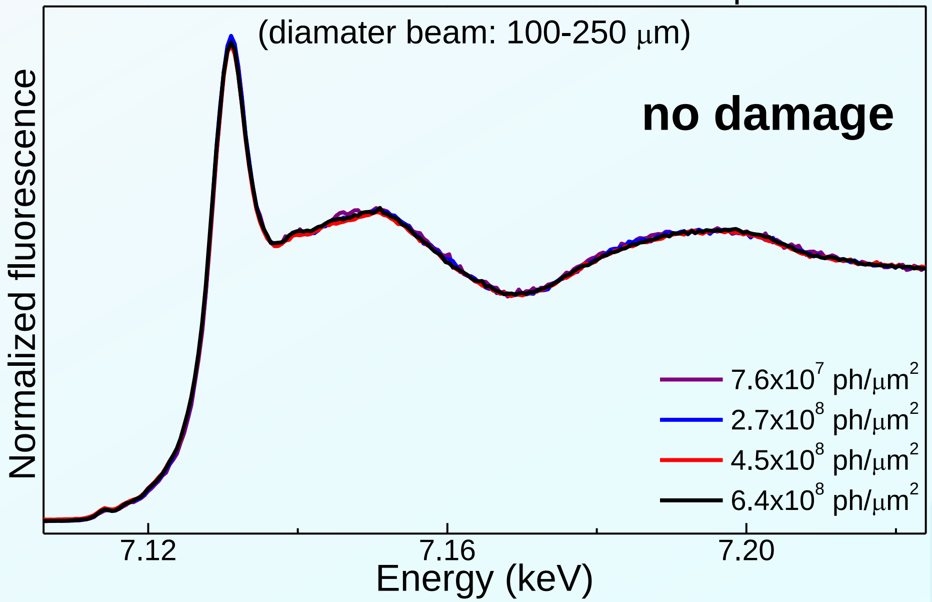

ID21

Focused mode- flux: 2×10^{9}-1×10^{10} ph/s

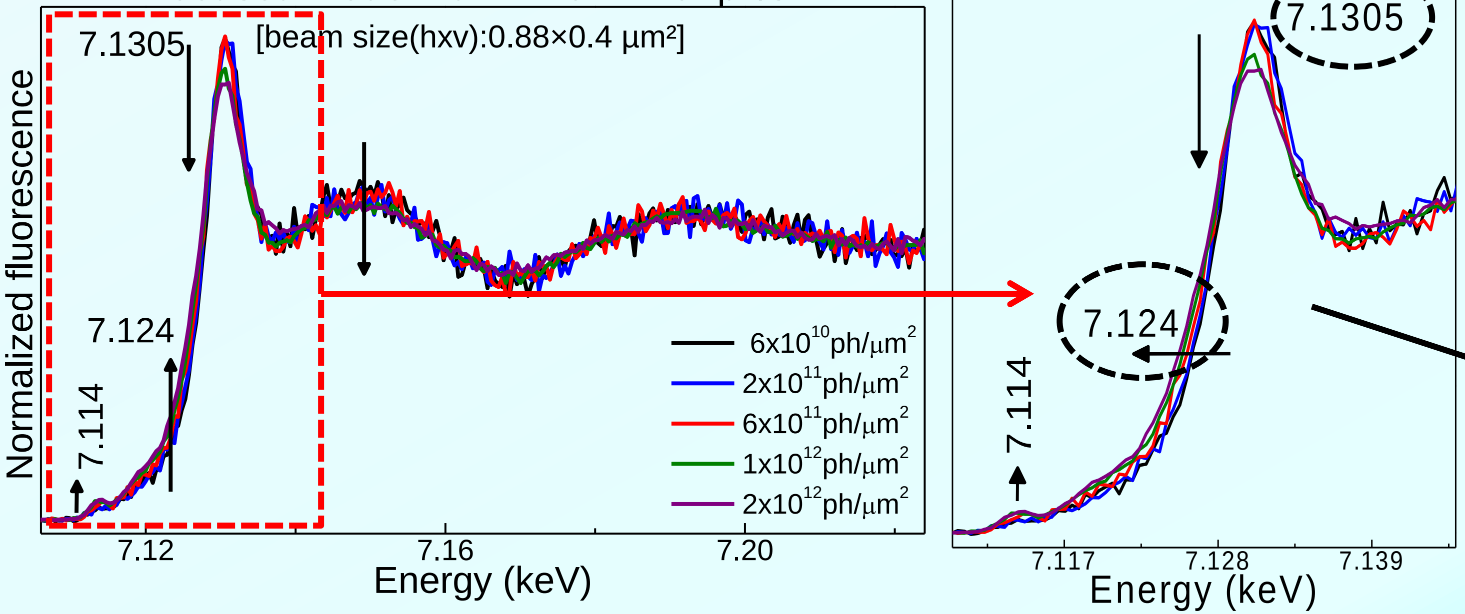

- Shift of the absorption edge toward lower energies

↓

$Fe^{III}\rightarrow Fe^{II}$ reduction

- Decreasing of the intensity of the white line at 7.1305 keV, and increasing of the intensity of pre-edge peaks

↓

greater disorder and deformation of the octahedral coordination sphere of Fe ions.[(a),(b)]

no damage up to ca. 2-3×10^{11} ph/μm²

Energies for 2D μ-XRF mapping selected by taking into account the variations induced by the exposure to the X-ray microbeam

[(a)] L. Samain *et al.*, *JAAS* 26 (2011) 930–941 and 28 (2013) 524–535; [(b)] C. Gervais *et al.*, *Langmuir* 31 (2015) 8168-8175.

5-PB faded paint cross-sections: multiple energies 2D µ-XRF mapping + single point µ-XANES at Fe K-edge

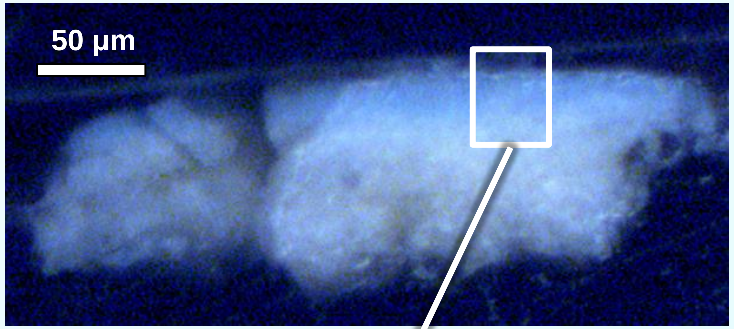

Step size (v×h): 0.3×0.5 µm²
Map size (v×h): 64.5×33 µm²
Exposure time: 100 ms/pixel
Fluence (3 energies): 1×10^{9} ph/µm²

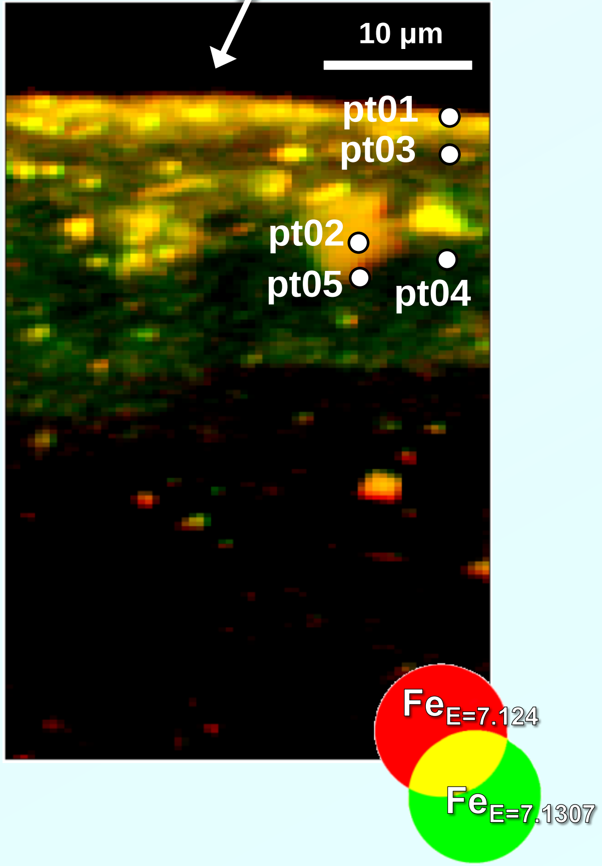

ID21
ESRF

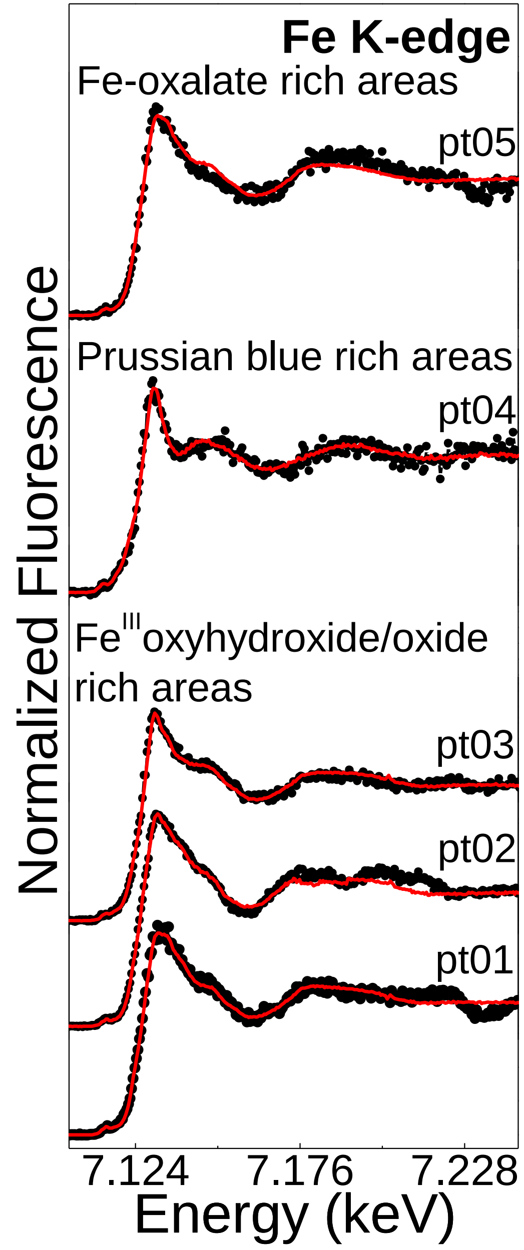

Fluence: 2-3×10^{11} ph/µm²

pt05:
Fe^{III}oxyhydroxide/oxide (gohetite/hematite)=(48±9)%
Fe^{II}/Fe^{III}-oxalate=(40±9)%
Prussian blue/$K_4Fe^{III}(CN)_6$=(12±2)%

pt04:
Fe^{II}/Fe^{III}-oxalate=(32±4)%
Prussian blue-aged/$K_4Fe^{II}(CN)_6\cdot3H_2O$=(68±7)%

pt03:
Fe^{III}oxyhydroxide/oxide (gohetite/hematite)=(70±7)%
Fe^{II}-oxalate=(10±2)%
Prussian blue/$K_4Fe^{II}(CN)_6\cdot3H_2O$=(20±2)%

pt02:
Fe^{III}oxyhydroxide (gohetite)=(85±2)%
Fe^{II}-oxalate=(15±2)%

pt01:
Fe^{III}oxyhydroxide/oxide (gohetite/hematite)=(88±7)%
Fe^{II}-oxalate=(5±2)%
Prussian blue=(7±2)%

Fe^{III} -oxyhydroxide
- deep natural fading of PB[(a)]
- residue of manufacture process[(b)]

[(a)] C. Gervais *et al.*, *Langmuir* 31 (2015) 8168-8175; [(b)] L. Samain *et al.*, *J. Synchrotron Rad.* 20 (2013) 460 – 473.

5-Fe K-edge XANES of reference compounds

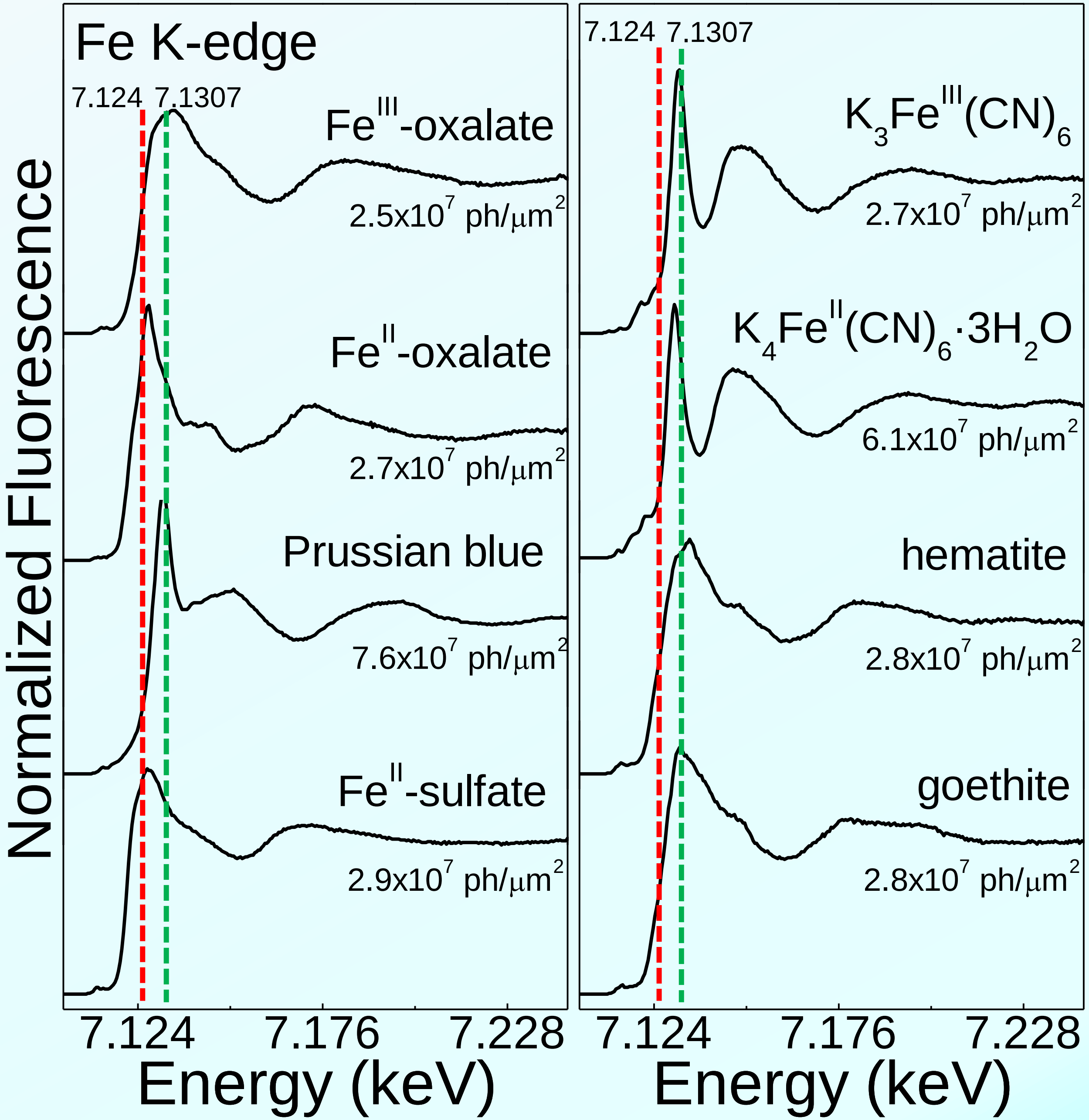

Selected energies not suitable for the selective excitation of either Fe^{II}- or Fe^{III} –species

ID21

ESRF

5-PB faded paint cross-sections: 2D μ-XANES mapping at Fe K-edge (XRF mode)

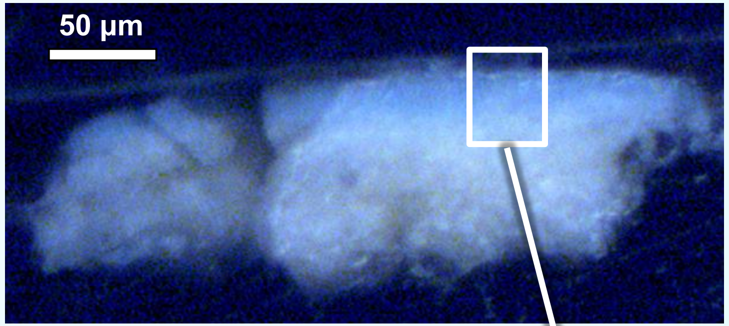

ID21

ESRF

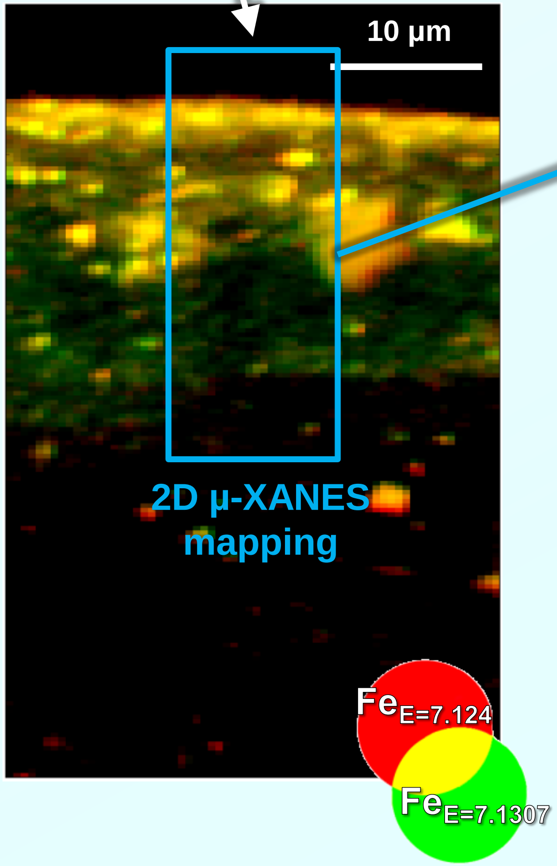

Step size (v×h):
0.3×0.5 μm^2
Map size (v×h):
64.5×33 μm^2
Exposure time:
100 ms/pixel
Fluence (3 energies):
1×10^9 ph/μm^2

Step size (v×h):
0.5×1 μm^2
Map size (v×h):
26.5×11 μm^2
Exposure time:
100 ms/pixel
Fluence (173 energies):
~2.5×10^{10} ph/μm^2

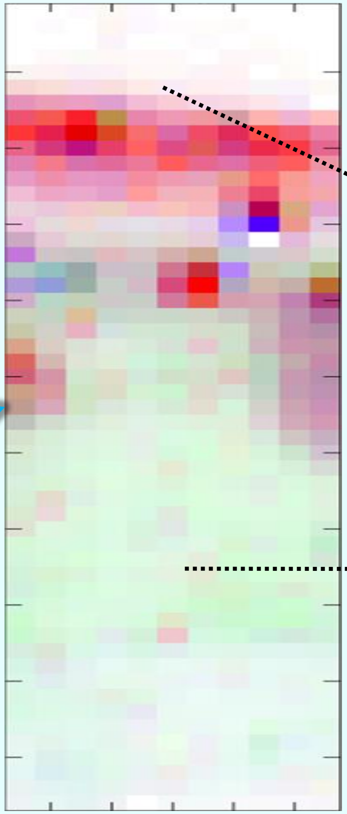

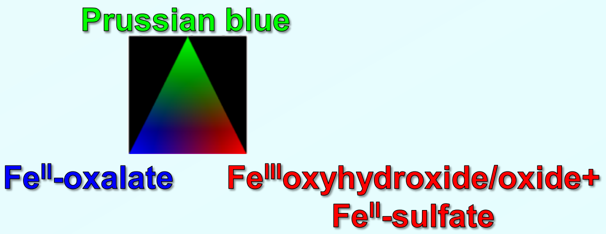

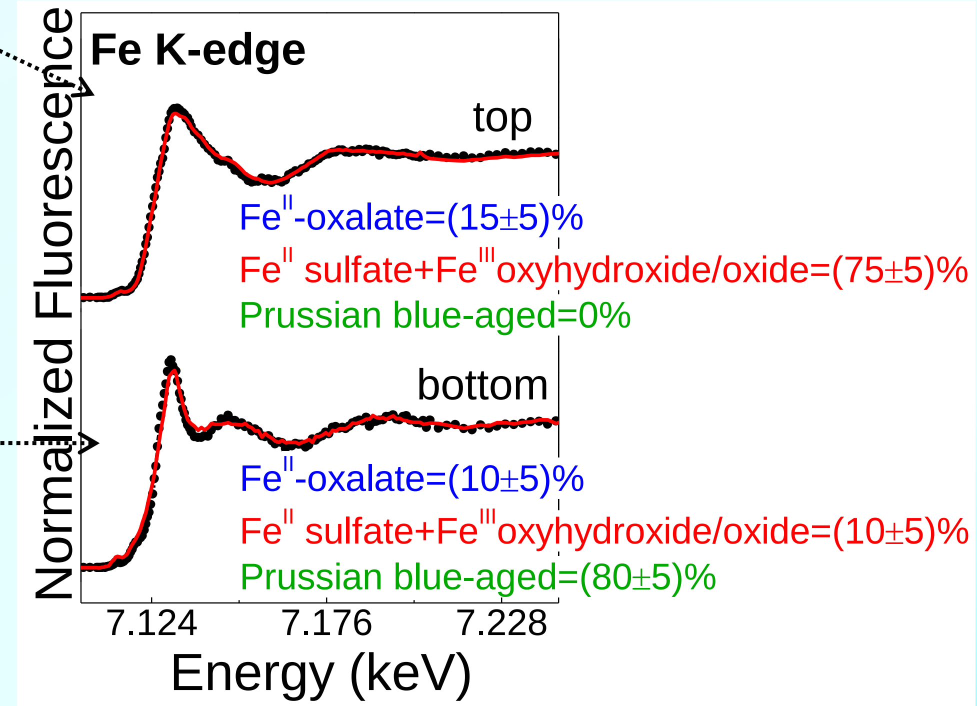

↑ More representative datasets (one XANES spectrum per pixel)
↑ Lower fluences (probability of beam damage decreased)
↑ Suitable for diluted samples
↑ No loss of spatial/lateral resolution
↓ Longer acquisition time

Best compromise among:
- Map size
- step size
- exposure time
- spectral resolution (n. energy maps)

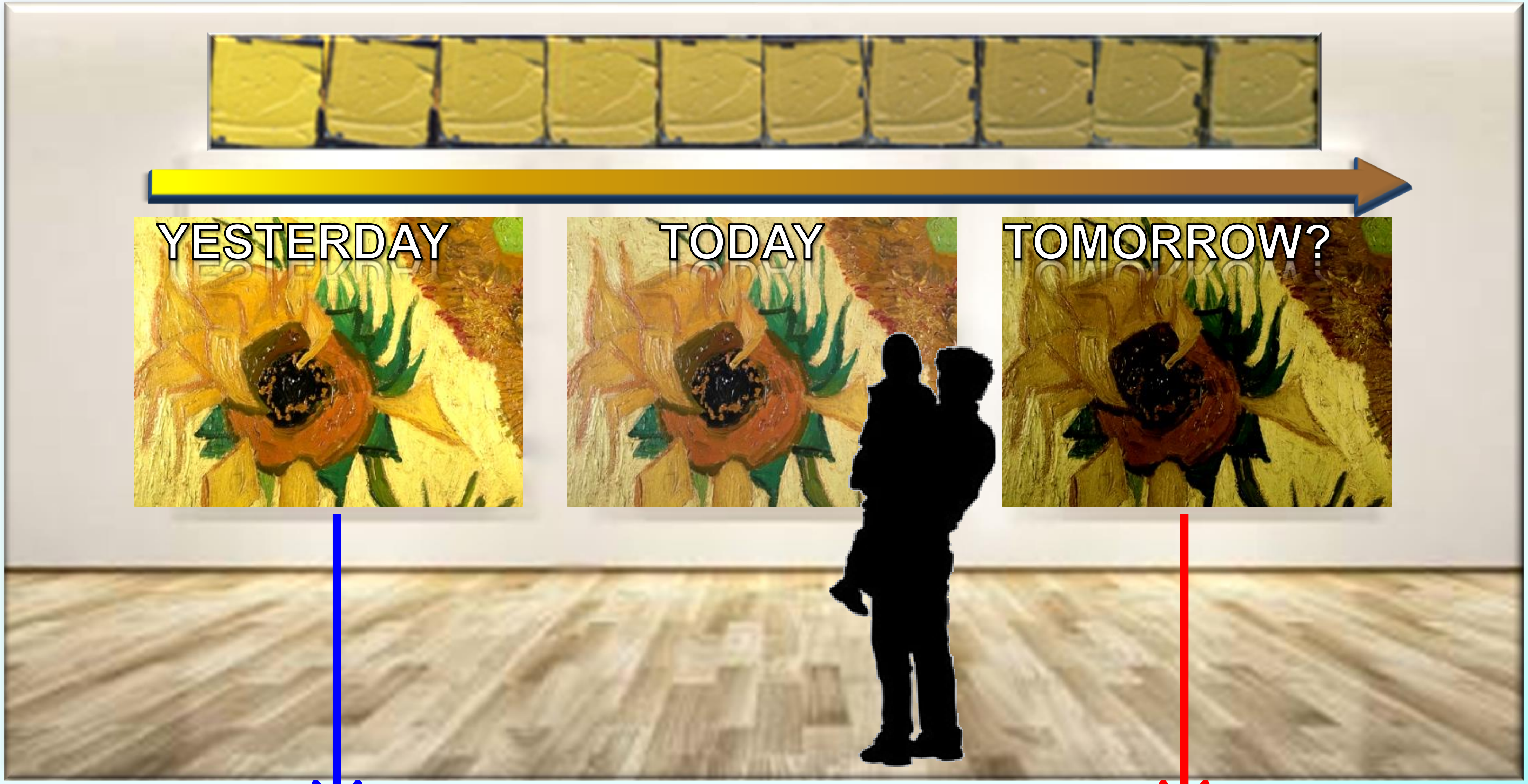

LOOKING BACKWARDS

how the painting looked from the moment it was finished?

LOOKING INTO THE FUTURE

What we can do now for preventing the degradation?

Acknowledgments

- A particular acknowledgment for the financial support from:

  - **IPERION-CH** (EU H2020-INFRAIA-2014-2015, Grant No. 654028)
  - **CHARISMA** (EU FP7 programme, Grant No. 228330)
  - **CALIPSOplus** (EU H2020-Research and Innovation, Grant No. 730872)
  - **AMIS**-Dipartimenti di Eccellenza 2018-2022 (funded by MIUR and University of Perugia)
  - **ESRF** (exps. EC-504, EC-799, EC-1051, HG-18, HG-26, HG-32, HG-64, HG-95, HG-98, HG107, HG-129 and in- house beamtimes)
  - **DESY-PETRA III** (exps. I-20130221 EC , I-20160126 EC, I-20160672 EC and I-20170721 EC)
  - **Australian synchrotron** (exp. M-4604)
  - **FWO (Brussels)** (projects no. G.0C12.13, G.0704.08, G.01769.09, G.0566.19N and G.0547.19N)
  - **BELSPO (Brussels)** “S2-ART“ (SD04A)
  - **GOA “SOLARPAINT”** (Research Fund Antwerp University: BOF-2015)
  - **Fund Inbev-Baillet Latour (Brussels)**

Van Gogh Museum Amsterdam

Rijksdienst voor het Cultureel Erfgoed
Ministerie van Onderwijs, Cultuur en Wetenschap

Kröller Müller museum

MUNCH MUSEET

CATS Centre for Art Technological Studies and Conservation

SMK Statens Museum for Kunst
National Gallery of Denmark